Research and Development Technical Report

ECOM-74-0587-F

INVESTIGATION OF HIGH TEMPERATURE BATTERY SYSTEMS

R. R. SAYANO
M. L. MCCLANAHAN
J. A. MALE
N. FRIED

TRW SYSTEMS GROUP
One Space Park
Redondo Beach, CA 90278

DECEMBER 1975

FINAL REPORT FOR PERIOD 1 JUL 74 – 31 AUG 75

Prepared for

ECOM

US ARMY ELECTRONICS COMMAND FORT MONMOUTH, NEW JERSEY 07703

NOTICES

Disclaimers

The findings in this report are not to be construed as an official Department of the Army position, unless so designated by other authorized documents.

The citation of trade names and names of manufacturers in this report is not to be construed as official Government indorsement or approval of commercial products or services referenced herein.

Disposition

Destroy this report when it is no longer needed. Do not return it to the originator.

Research and Development Technical Report

ECOM-74-0587-F

INVESTIGATION OF HIGH TEMPERATURE BATTERY SYSTEMS

R. R. SAYANO
M. L. MCCLANAHAN
J. A. MALE
N. FRIED

TRW SYSTEMS GROUP
One Space Park
Redondo Beach, CA 90278

DECEMBER 1975

FINAL REPORT FOR PERIOD 1 JUL 74 – 31 AUG 75

Prepared for

ECOM

US ARMY ELECTRONICS COMMAND FORT MONMOUTH, NEW JERSEY 07703

ABSTRACT

Hermetically sealed sodium-sulfur cells intended to operate at 300 °C in atmospheric environment and to deliver 10 A for 2 hr above 1.0 V for 100 cycles with a specific power and specific energy of 110 W/kg and 110 W hr/kg, respectively, were designed and fabricated. The cells were to withstand five thermal cycles from operating temperature to room temperature without loss of electrical performance. These cells utilized a disk shaped magnesium oxide-enriched β-alumina electrolyte with low cost materials for cell containers.

The seals used in the cell were all based on state-of-the-art technology and comprised a glass sealant between the β-alumina electrolyte and the α-alumina rings, copper braze between the α-alumina rings and the Kovar cell containers, and laser welds between the Kovar cell containers and the stainless steel cell cover. Chromium plasma coating was used to protect the copper braze and Kovar against corrosion by sulfur and/or sodium polysulfide. No catastrophic cell failure due to cell design or materials of construction has been observed during testing of a cell for over 800 hr.

A cell has been electrically cycled for 57 cycles (over 800 hr) with a coulombic efficiency greater than 90% without any sign of performance degradation. In addition the cell has undergone five thermal cycles from operating temperature to room temperature and back to operating temperature without exhibiting any loss of performance. The projected performance of the cell at the 10-A discharge rate is 112 W/kg and 224 W hr/kg for specific power and specific energy, respectively. However, due to high internal resistance, the cell could not be discharged at currents greater than 3 A while maintaining the operating voltage above 1.0 V. The maximum specific energy was 310 W hr/kg and the specific power at maximum power (3-A current) was 16 W/kg.

CONTENTS

LIST OF TABLES

LIST OF FIGURES

LIST OF FIGURES

1. INTRODUCTION

A program for design and construction of rechargeable hermetically sealed sodium-sulfur solid-electrolyte cells capable of operating in an atmospheric environment was undertaken for the United States Army Electronics Command (USAECOM), Fort Monmouth, New Jersey. The cells are designed to provide high transient pulse power on a prescribed duty cycle and meet or exceed the following performance characteristics:

- Operating temperature of less than 380 °C
- Specific power of no less than 50 W/lb
- Specific energy of no less than 50 W hr/lb
- Capacity of no less than 20 A hr when discharged at the 2-hr rate to a cut-off voltage of 1.0 V
- Coulombic efficiency of no less than 90%
- Charge-discharge cycle life of no less than 100 cycles
- Thermal cycle life of no less than 5 cycles (cooling from operating temperature to 25 °C in 30 hr followed by reheating to operating temperature in 10 hr, maintaining at operating temperature for 24 hr and discharging at the 2-hr rate).

The results of the program leading to the fabrication and evaluation of hermetically sealed cells are presented in the following sections.

2. RESULTS

2.1 Characterization of Sodium Aluminate Solid Electrolyte. The requirements for the solid electrolyte for sodium-sulfur cells are often repeated and quite straightforward. Simply stated, the material must be simultaneously strong, conductive, and inexpensive and must possess a long service life. The development of such a material is less straightforward because it entails the selection of a composition (thus a crystalline structure) and a fabrication method, both from myriad possibilities.

Two distinct compositions, magnesium oxide-enriched β-alumina and lithium oxide-stabilized β"-alumina have been the subject of TRW's work. In the single crystal structures of β-alumina and β"-alumina, the idealized backbone structure of the oxygen and aluminum ions are the same. It is only in the stacking order of the close-packed oxygen planes, and the coordination of available sodium sites resulting from the stacking order, that differences are noted. The two forms are, however, quite different in terms of properties. The β-alumina material is more resistive (10-12 Ω cm at 300 °C) but is readily prepared with the uniform fine microstructure which is necessary for high strength. The β"-alumina has a lower resistivity (3-6 Ω cm at 300 °C) but exhibits a marked tendency to form exaggerated grains during sintering.

2.1.1 Isostatically Pressed Magnesium Oxide-Enriched β-Alumina. Uniaxial precompaction and isostatic pressing followed by sintering is the technique which has been most successful in producing high quality solid electrolyte. Magnesium oxide-enriched β-alumina disks produced by this method have exhibited very desirable physical characteristics. Electrolytes were characterized with respect to density, microstructure, strength, and conductivity. Electrolyte plates formed by this method had an average density of 3.24 g/cm^3 and were found to have uniform microstructure throughout. Figure 2-1 is a scanning electron micrograph showing a typical microstructure of these β-alumina plates. These plates have an equiaxed grain structure with a grain diameter of about 3 μm and a porosity of 1-2 vol % resulting in a strength of 2.6 × 10^4 psi (1.8 × 10^8 Pa) and an elastic modulus of 4.5 × 10^7 psi (2.8 × 10^{11} Pa). Material of this type typically exhibited a sodium ion resistivity at 300 °C of 11-15 Ω cm and an activation energy of 6-7 kcal/mol (25-27 kJ/mol). The Arrhenius plot for a typical sample is shown in Figure 2-2 and Table 2-1 presents some of this data.

2.1.2 Isostatically Pressed Lithium Oxide-Stabilized β"-Alumina. Because of our previous successful experience with uniaxial precompaction followed by isostatic pressing, this forming method was chosen for the initial experiments with lithium oxide-stabilized β"-alumina. However, this work is not as advanced as comparable studies involving β-alumina.

Those disks produced exhibited a density of 3.17 g/cm^3 and were impermeable to helium. This composition produced disks with low resistivity, however, the grain size of this material is more difficult to control than that of mangesium oxide-enriched β-alumina. An example of the sort of exaggerated grain growth which was encountered is shown in Figure 2-3.

Table 2-1. Resistivity as a Function of Temperature for Magnesium Oxide-Enriched β-Alumina

Temperature, °C	Resistivity, Ω-cm
350	[illegible]
300	11.[illegible]
250	1[illegible]
200	29.[illegible]
150	55.6
100	136

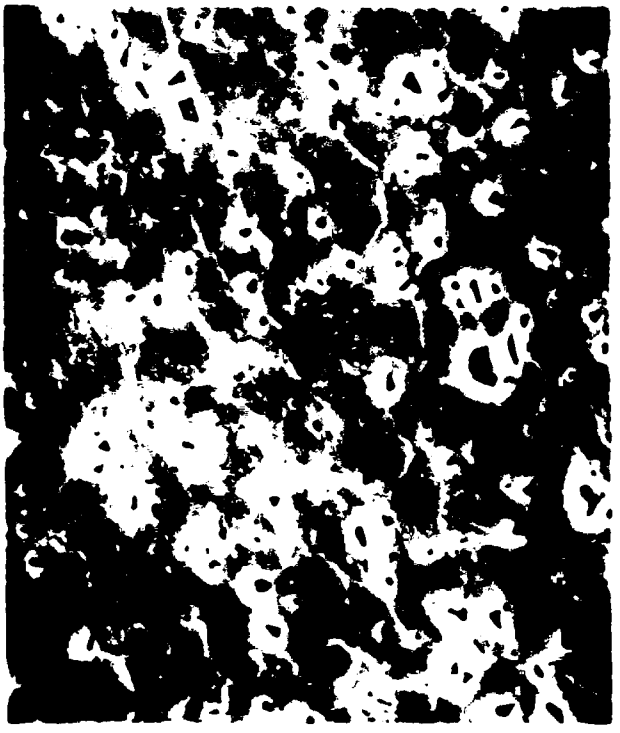

Figure 2-1. Scanning Electron Micrograph of Magnesium Oxide-Enriched β-Alumina Disk Prepared by Isostatic Pressing and Sintering (2000×)

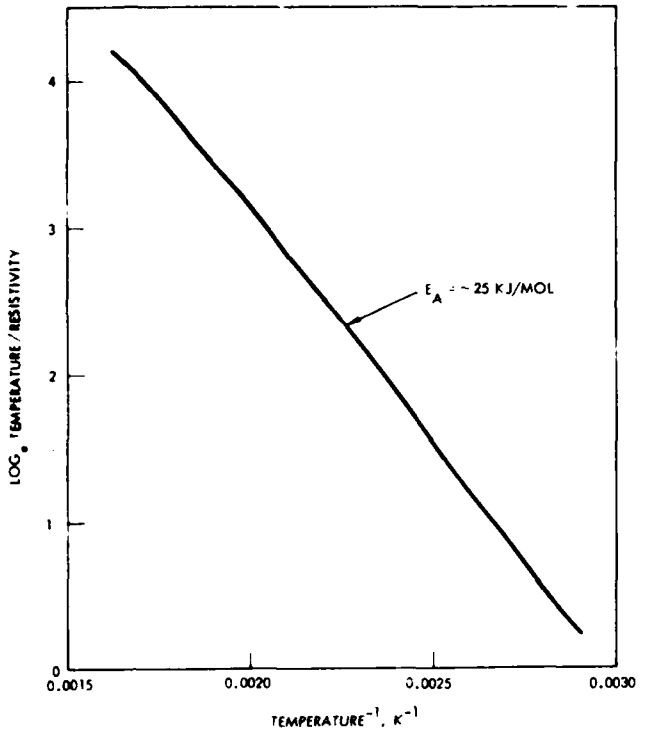

Figure 2-2. Arrhenius Plot of Cold-Pressed Magnesium Oxide-Enriched β-Alumina

Figure 2-3. Scanning Electron Micrograph of a Sample of Lithium Oxide-Stabilized β"-Alumina (100×)

The resistivity of this material was 4.5 Ω cm at 300 °C and the activation energy in the low temperature region was 7.0 kcal/mol (29 kJ/mol). The Arrhenius plot is shown in Figure 2-4 and some of the data is presented in Table 2-2. The fracture strength of this material was determined from burst tests of 2.0-cm diameter disks of 0.015-cm thickness and found to range between 1.0×10^4 psi (6.9×10^7 Pa) and 2.4×10^4 psi (1.6×10^8 Pa). This was consistent with the observation of several exaggerated grains in scanning electron micrographs of this material.

Table 2-2. Resistivity as a Function of Temperature for Lithium Oxide-Stabilized β"-Alumina

Temperature, °C	Resistivity, Ω cm
350	3.91
300	4.51
250	5.75
200	8.31
150	14.9
100	36.6
50	68.4

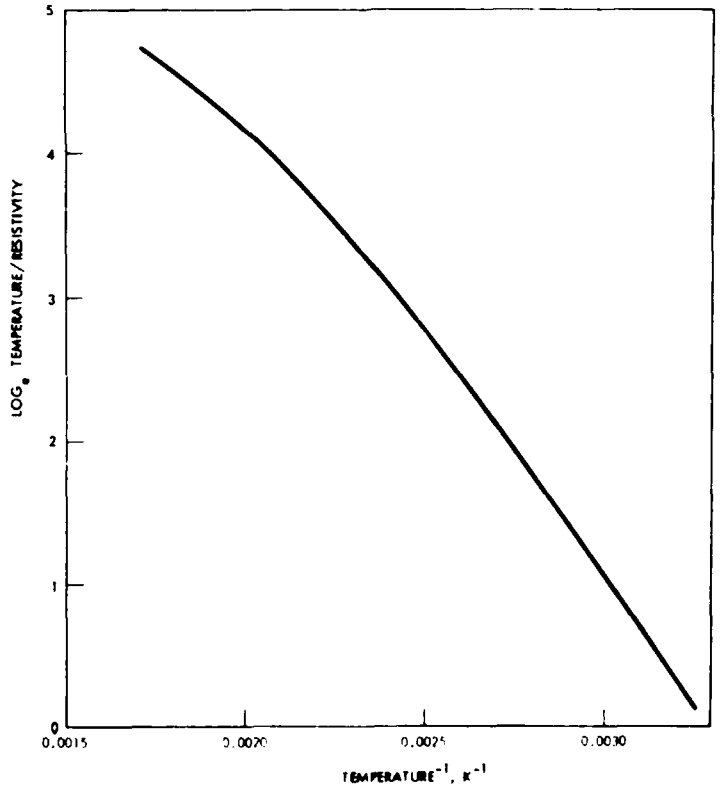

Figure 2-4. Arrhenius Plot for Lithium Oxide-Stabilized β"-Alumina

2.1.3 Hot Pressing of Sodium Aluminate Solid Electrolyte. During the early stages of the TRW Advanced Batteries Program considerable success was enjoyed with solid electrolyte assemblies machined from hot-pressed β-alumina. The material produced at that time was a very dense (as high as 3.27 g/cm^3) magnesium oxide-enriched β-alumina. The resistivity of this material was 30 Ω cm at 300 °C with an activation energy of 6.7 kcal/mol (28 kJ/mol). The microstructure was encouragingly fine and the flexure strength was quite high (3.7×10^4 psi or 2.59×10^8 Pa). However, when the production of higher quality isostatically pressed and sintered magnesium oxide-enriched β-alumina described in Section 2.1.1 became routine, the development effort on hot-pressed materials was discontinued.

2.2 Selection of Solid Electrolyte Formulation and Fabrication Procedure. Uniaxial precompaction followed by isostatic pressing and sintering was selected as the best method for fabricating 7.6-cm diameter solid electrolytes for this program. This method results in solid electrolytes which have a high density and are more uniform than those fabricated by uniaxial pressing and sintering or by hot pressing. Therefore, fabrication of disks for the deliverable cells was done by this method.

Magnesium oxide-enriched β-alumina was selected as the electrolyte composition due to its demonstrated long-term stability in sodium-sulfur test cells. The resistivity of this material (10-12 Ω cm at 300 °C) is adequate for cells meeting the performance requirements of this program; however, in other programs alternate compositions which can result in electrolytes with lower resistivity and long-term stability were investigated.

2.3 Evaluation of Seals. In addition to the welding procedures used to make the final closures of the hermetically sealed cells, metal-to-ceramic seals and seals between α-alumina and β-alumina are also required. Ceramic-to-metal seals fabricated by commerically available techniques were evaluated along with materials of construction in tests which are described in Section 2.4.

In the cell design of the previous USAECOM program, a glass seal was made between two interlocking β-alumina cups. This configuration had the advantages of self-alignment and minimized thermal expansion differences. Although the seals worked, they were difficult and costly to produce and structural flaws introduced during the required machining of the ceramic cups resulted ultimately in failure of the β-alumina cups. Thus, ceramic-to-ceramic seal development has continued and many improvements have been made.

Figure 2-5 is a schematic of a new double ring-disk seal design showing α-alumina rings sealed to both sides of the β-alumina electrolyte to minimize stresses. The α-alumina rings are attached to the metallic cell containers by standard ceramic-to-metal sealing techniques. The development and qualification of this seal involved characterization of sealants (development of time-temperature schedules for firing) and the adaptation of sealing schedules for the production of hermetically sealed cells.

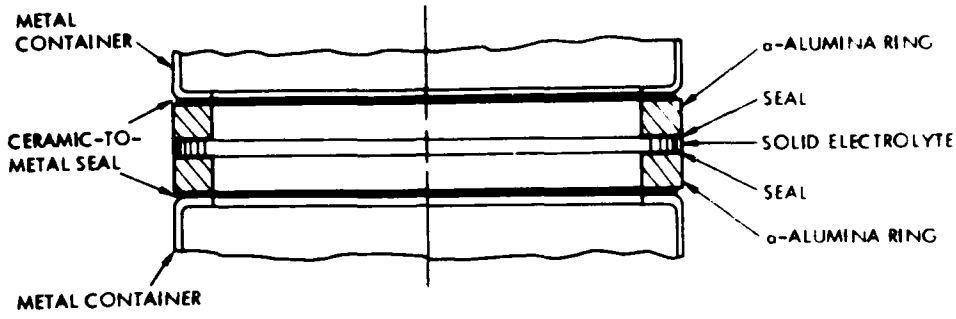

Figure 2-5. Schematic of α-Alumina-to-β-Alumina Seal

2.3.1 Characterization of Sealing Glasses. Two sealing materials which had previously been shown to be sodium resistant were selected for further development and evaluation. One material was a borosilicate glass with appropriate thermal expansion characteristics and the other was a commercial glass sealing formulation which consisted of glass, additives, binder, and solvent. The glass component was the same in both materials. Seals between sections of α-alumina tubing were made using these materials in the early work to develop sealing schedule. The tubing used was 1.9-cm o.d. Coors AD-998 α-alumina tubing which had been centerless ground.

The surfaces to be sealed were ground flat and parallel and provided with a 40-μin. finish. All of the pieces were cleaned ultrasonically in hexane for 10 min and air dried. A thin strand of sealing paste was applied to one of the pieces, and the other piece was positioned on the coated face and rotated about one-eighth turn back and forth two times. The assemblies were carefully aligned and maintained at 70 °C for 30 min (or 130 °C for 25 min) in a convection oven to remove the solvent prior to firing.

The first tube-to-tube assemblies made using the commercial glass formulation were fired using a conventional sealing schedule. Examination of the cross sections of these seals revealed that very little glass had remained between the two sections of tubing. In addition many large bubbles and voids were observed in the sealant. This indicated that the glass had been allowed to become too fluid and/or the pieces were too heavily loaded during firing. In future experiments care was taken to avoid putting pressure on the seal during the assembly process, the sealing jig was modified to lessen the load on the seal during the firing cycle, and temperatures lower than 1060 °C were used.

Using the above results as a guideline, an experiment was designed to provide information which could be used to optimize the firing schedule. The solvent removal step and the low temperature binder burnout schedule were the same for all samples while the time and temperature were varied for the sealing step (0.5 and 2.0 hr at 750 and 850 °C). The

evaluation of seals prepared in this experiment involved:

1. Preliminary visual inspection
2. Determination of porosity with a helium-leak detector
3. Examination with a scanning electron microscope (SEM) and light microscopy
4. Tensile testing to measure the mechanical strength of the seal.

Of these techniques the latter two provided the most information.

Tensile testing revealed that seal strength increased with both increasing time and temperature. The results for the commercial glass formulation are shown in Table 2-3. The seals made with the sealing glass alone were only 20-40% as strong as those seals reported in Table 2-3. Examination of the fracture surfaces produced during tensile testing was also informative. The glass-to-alumina seals remained intact with the fracture occurring through the glass. SEM examination of the fracture surfaces generally showed the presence of many small bubbles in the interior of the glass, channels parallel to the circumference of the tube, and a few bubbles near the outer edges. Figures 2-6 and 2-7 are examples of this behavior.

Table 2-3. Ultimate Tensile Strength of Ceramic-to-Ceramic Seals Prepared with Commercial Sealing Glass Formulation

Sealing Temperature, °C	Sealing Time, hr	Ultimate Tensile Strength × 10^{-3}, psi
750	0.5	4.9
750	2.0	9.8
850	0.5	11.6
850	2.0	13.1

The results obtained by SEM were very much dependent upon sample preparation. Metallographic polishing techniques using diamond paste accompanied with frequent examination with a light microscope were found to produce the most meaningful results. Other techniques which were used to prepare the surface usually masked or destroyed much of the information. Acid-etching procedures seemed to remove the glass quite readily and etching appeared to occur preferentially at the ceramic-to-glass interfaces, thus making observation of the interface impossible. Techniques commonly used for polishing ceramic samples were also evaluated for preparation of the cross-sectional samples, but in many cases small voids were filled in and seemed to disappear.

Information obtained by the SEM included data bearing upon:

1. Preliminary visual inspection

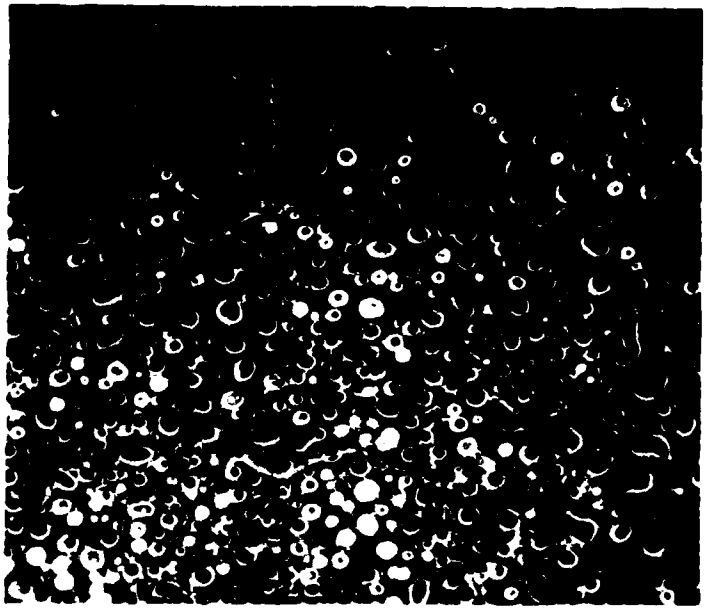

Figure 2-6. Scanning Electron Micrograph of the Interior Section of the Fracture Surface of a Ceramic-to-Ceramic Seal (100×)

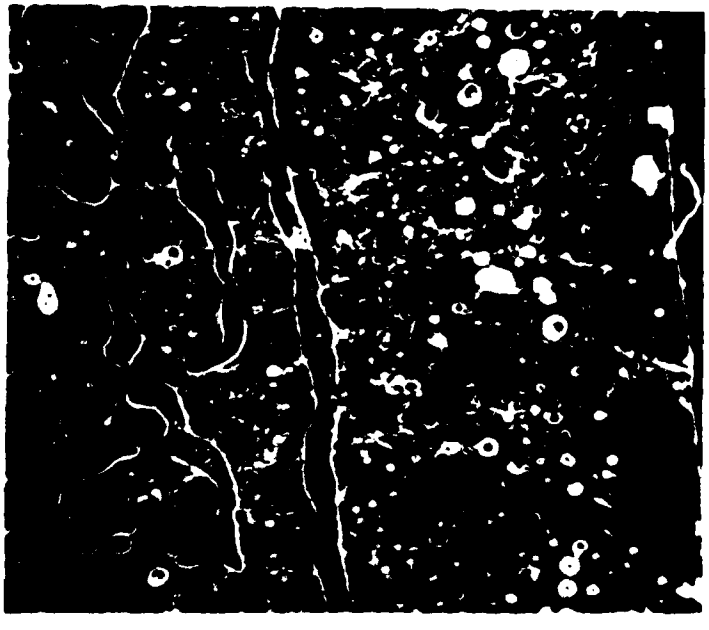

Figure 2-7. Scanning Electron Micrograph of the Exterior Section of the Fracture Surface of a Ceramic-to-Ceramic Seal (100×)

2. Number of voids

3. Size of voids

4. Size of glass fillet

5. Contact angle between the glass and ceramic.

Figures 2-8 and 2-9 are examples of the micrographs obtained in the course of this study. The seals shown in these figures are the same ones for which tensile strengths are reported in Table 2-3. The most important observation to be made from these micrographs is the dependence of the glass-to-ceramic contact angle upon firing schedule.

These results provided information essential to the fabrication of sealed assemblies for working cells in that they:

1. Identified a sealant (the commercial preparation was used in all subsequent work)

2. Established both the range and effect of firing conditions

3. Provided experience with various techniques of seal evaluation.

An electrochemical evaluation of the commercial glass formulation and the double ring-disk seal configuration was carried out by constructing and operating a tubular laboratory test cell which utilized a 1.9-cm diameter α-alumina tube-to-β-alumina disk-to-α-alumina ring anode assembly. The cell was thermally cycled once and operated for a total of 1100 hr at 300 °C. The testing was terminated when the cell voltage dropped suddenly. The cell underwent 53 cycles (250-mA discharge for 0.75 hr, 250-mA charge for 2 hr with 2.5-V limit) for a total charge of 10 A hr. Disassembly of the cell revealed evidence of an anode leak to the atmosphere and cracks in the α-alumina tube. There was no evidence that cell failure was due to failure of the ceramic-to-ceramic seal although helium leak testing after disassembly indicated some seal leakage.

To develop the techniques necessary for fabricating larger assemblies, several seal assemblies were fabricated from 7.6-cm diameter by 0.15-cm thick β-alumina electrolytes and α-alumina rings with a 0.63-cm or 0.32-cm square cross section. One such seal assembly with 0.63-cm cross section rings underwent three thermal cycles between about 50 and 350 °C without any degradation of seals, electrolyte or rings. The temperature was varied at a rate of about 70 °C/hr which was quite a bit higher than the required heat-up and cool-down rates of 30 °C/hr and 10 °C/hr, respectively. This type of seal was evaluated further in a boiler-plate cell described in Section 2.7.2.

2.3.2 Hermetically Sealed Cells. The restrictions placed upon the sealing conditions in the case of assemblies for boiler-plate cells are quite simple. They involve only the avoidance of temperatures which could cause sodium oxide loss from the β-alumina and the adherence to

Figure 2-8. Scanning Electron Micrograph of a Cross Section of a Ceramic-to-Ceramic Seal. The sealing schedule was 30 min at 750 °C (40×)

Figure 2-9. Scanning Electron Micrograph of a Cross Section of a Ceramic-to-Ceramic Seal. The sealing schedule was 2 hr at 850 °C. The two α-alumina tubes are offset resulting in the unusual appearance (40×)

temperature change rates which minimize thermal stresses. For the fully sealed cells the problem is more complex because the α-alumina ring has been brazed to a metal subassembly. The problems introduced by the metal subassembly are associated with:

1. The presence of more severe thermal mismatches
2. The oxidation of the metal at temperatures above 500 °C
3. The maximum temperature which the braze will survive (1000 °C).

These conditions must in some way be reconciled with the requirements of the glass sealant which include:

1. Binder burnout in an oxidizing environment
2. An optimum fusion temperature of 1150 °C

A schedule was developed which appears to satisfy the requirements of the sealant and the metal components. The schedule used heating and cooling rates of 25 °C/hr with flowing oxygen at temperatures below 500 °C and an argon atmosphere at higher temperatures. Details of the sealing procedure are provided in Section 2.6.2.

2.4 Evaluation of Materials of Construction. The basic materials of construction for the hermetically sealed cells are solid electrolyte, α-alumina, Kovar and stainless steel. Most of these materials have been examined in TRW's IR and D program and under the previous USAECOM program and no serious compatibility problems have been seen in the lifetimes of the cells operating at the temperatures of interest.

However, further evaluation of materials of construction under actual cell operation was necessary in order to determine the extent and type of corrosion and its effects of cell performance. The materials of construction for hermetically sealed sodium-sulfur cells were evaluated in a boiler-plate test cell. The samples which were imbedded in the sulfur cathode felt included corrosion test coupons and samples of ceramic-to-metal seals.

2.4.1 Ceramic-to-Metal Seals. Two types of commercially available ceramic-to-metal seals were evaluated. The first type was prepared by the molybdenum-manganese metallization technique. The technique involves metallization of α-alumina with molybdenum-manganese alloy and is used widely in the high vacuum and electronic industries. A molybdenum-manganese mixture is coated onto a pretreated surface of α-alumina and sintered under a wet hydrogen atmosphere. Since normal brazing materials do not adhere very well to the metallized layer, a coating of nickel or copper is then applied by electroplating. A standard braze material is finally used to seal the metal to the metallized ceramic. The metal is selected so that its thermal expansion behavior is similar to the α-alumina in order to minimize thermal stresses.

The second type of seal considered was fabricated by active metal brazing. This method involves sealing the metal directly to α-alumina with an active metal, such as titanium, zirconium, tantalum or niobium. The seal is typically made on ultrapure α-alumina and to prevent oxidation of the metal a high vacuum or an oxygen-free atmosphere is required for brazing.

Both of these techniques produce ceramic-to-metal seals that satisfy the requirements for sodium-sulfur cells. In order to evaluate the ceramic-to-metal seals more fully, samples of the seals made by both techniques were obtained from several commercial sources and were subjected to actual cell operating conditions. The evaluation consisted of placing the sample seals in a boiler-plate test cell (Section 2.7.2) and examining the condition of the seals after exposure to cell operation at 345 °C for 480 hr. The samples chosen and their sources are given in Table 2-4.

Table 2-4. Ceramic-to-Metal Seal Samples

Sample	Seal Type	Source
1	Kovar sealed to 99.5% α-alumina by copper alloy braze on molybdenum-manganese metallization.	Ceradyne, Inc.
2	Gold-plated Kovar sealed to α-alumina by copper alloy braze on molybdenum-manganese metallization.	3M Co.
3	Nickel sleeve sealed to 99.5% α-alumina rings in sandwich configuration by active metal braze.	ILC

The most serious chemical compatibility problem exists on the cathode rather than the anode side. Although our laboratory test cells have demonstrated that Type 300 series stainless steels behave acceptably when in contact with sulfur and sodium polysulfides for hundreds of hours, they cannot be used to make a ceramic-to-metal seal due to their large thermal expansion coefficient mismatch with α-alumina. Materials such as Kovar or Rodar whose thermal expansion coefficients are closely matched to that of α-alumina are typically used with α-alumina but these materials have relatively high corrosion rates in the sulfur-sodium polysulfide mixture (R.R. Dubin, 147th National Meeting, The Electrochemical Society, Toronto, May 1975, Extended Abstracts, p. 27). In addition, the common braze materials themselves are not well characterized in the cathode environment.

The exposure of Samples 1, 2, and 3 in the cathode compartment of a test cell (for a total of 480 hr at 345 °C - including 11 charge-discharge cycles with discharge currents as high as 10 A) were consistent with results obtained on our test coupons as well as with the results of others. Although only a moderate amount of surface corrosion was evident on Kovar, a cross-sectional view revealed a substantial amount of exfoliation indicating the formation of a nonprotective layer. A general attack of the copper braze material was also noted in metallized seals (Samples 1 and 2).

The active metal seal (Sample 3) did not reveal any gross corrosion either on the nickel sleeve or braze joint and appeared to represent a promising sealing technique.

The components of the commercially available ceramic-to-metal seals have been previously demonstrated to be compatible with molten sodium and were therefore not tested in sodium. However, a commercially available metallized alumina ring was evaluated for its compatibility with sodium. The ring was supplied by Alberox and was fabricated from 94% alumina (balance, silica). It was coated with molybdenum-manganese metallization on its sealing surfaces and was glazed on the other surfaces. This sample was tested with the hope that the protective coating would allow the use of a lower purity alumina which would be less expensive and easier to use. However, the exposure of this sample to molten sodium for 208 hr (with two thermal cycles between 100 and 300 °C) resulted in the α-alumina becoming brittle even though the metallization and the glaze on the outer surfaces of the ring appeared resistant to molten sodium. The results of this test clearly indicated the necessity of using higher purity alumina which is resistant to molten sodium.

2.4.2 Test Coupons. Additional materials evaluated were Type 304 and 304L stainless steel, Kovar and palladium-copper-silver braze alloy. The boiler-plate cell was operated for a total of 480 hr at 345 °C and underwent 11 electrical discharge/charge cycles. The test specimens were all retrieved intact from the boiler-plate cell. Visual observations indicated no gross corrosion of the test specimens. The specimens were cleaned with solvent and hot water to remove the polysulfide and sulfur, dried and weighed. Type 304 and 304L stainless steel and Kovar showed only a slight weight change. The palladium-copper-silver braze alloy was very brittle and showed a large weight loss.

Metallurgical examination of both Type 304 and 304L stainless steel revealed very little corrosion on the surfaces; however, a cross-sectional view revealed a substantial amount of exfoliation which indicates formation of a nonprotective scale and confirms the results observed with the ceramic-to-metal seal samples.

2.4.3 Selection of Materials. The results of these experiments clearly indicate that both Type 304 and 304L stainless steel are satisfactory materials for construction of sodium-sulfur cells. On the other hand, Kovar and the copper braze material which are necessary for the α-alumina-to-metal seal cannot be used without a protective coating. Nickel and chromium are possible coating materials that offer both corrosion resistance to the active materials and good electrical conduction. Clearly the active metal braze was the most attractive from the standpoint of chemical compatibility; however, several reasons precluded its use in the present instance. Foremost among these were:

- Noncritical parts - The metal and α-alumina parts do not have to be precision machined or ground. The α-alumina rings can be made from readily available extruded tubes. Since the seal is a butt seal the only requirement is that

the seal surfaces be flat. The active metal braze requires a sandwich configuration in which the metal is butt sealed between two α-alumina rings. This configuration is necessary to minimize unbalanced stresses in the seal. Therefore the α-alumina rings must be of exact dimension and geometry to insure proper alignment of parts.

- o Simplicity of jigging and tooling - Since the parts do not have to be precisely aligned, jigging and tooling are simplified.

- o Low cost - The cost for parts is low since standard fabrication techniques are used. The α-alumina does not have to be custom fabricated.

- o Minimum delivery time - Since the metallization technique is a standard ceramic-to-metal sealing method, multiple sources are available.

In order to effect the compromise between chemical compatibility and ready availability it was necessary to provide a protective coating to the cathode side of the α-alumina-to-metal seal. Chromium has been shown to be resistant to the sulfur-sodium polysulfide environment and was chosen for this purpose.

2.5 Design of Battery. A design of a hermetically sealed sodium-sulfur cell capable of meeting or exceeding the performance requirements was established from an engineering design analysis similar to that carried out for the previous USAECOM-supported program. The analysis consisted of:

- o General computer modeling studies to define the relationship between the solid electrolyte thickness and diameter

- o Consideration of engineering feasibility and fabrication techniques

- o Consideration of alternative designs to ensure safe and timely construction of the cells.

Computer modeling studies showed that the performance objectives can be met by a single cell utilizing an electrolyte of either tubular or flat-plate geometry. The flat-plate geometry was chosen based on the potential application of the battery system and appears to offer the following advantages over the tubular geometry:

- o Cells capable of being stacked in either series or parallel configurations depending on the service requirements for the battery system

- o Ease of thermal control of individual cells

- o Ease of low-cost fabrication of solid electrolyte using conventional equipment

- o Feasibility of developing a nondestructive test for quality control during cell fabrication
- o Cells easily packaged into a high density battery
- o Choice of hot-pressed, uniaxially pressed and sintered, isostatically pressed and sintered solid electrolytes.

The baseline cell design resulting from the engineering design analysis is shown in Figure 2-10. The major improvements in this design compared to the design developed in the previous program are:

- o The use of single cathode design utilizing solid electrolyte with resistivity of 10 .. cm at 300 °C
- o The use of the double ring-disk seal between the solid electrolyte and α-alumina rings to minimize unbalanced stresses in the seal and electrolyte and to provide electrical insulation to prevent electrochemical leakage during charging
- o Elimination of intricate and costly machining of the electrolyte
- o The use of a flat-plate solid electrolyte produced by a conventional fabrication method (hot pressing, uniaxial pressing and sintering, isostatic pressing and sintering)
- o Elimination of the complex anode fill-tube/current-collector assembly
- o Elimination of the anode fill-tube/current-collector feed-thru in the anode (ceramic) housing
- o Cell fabrication and assembly procedures that can be scaled up to large quantity, low cost production.

The assumptions and considerations used in the engineering design analysis in many cases reflected recent improvements in solid electrolyte and sodium-sulfur cell technology. These assumptions follow.

- o The designed capacity was 23 A hr since data from laboratory test cells indicated better than 90% utilization of active materials and a coulombic efficiency of 100%.
- o The cell was designed to operate at 300 °C to minimize materials compatibility problems which are encountered at higher temperatures of operation. Laboratory test cell data indicated no apparent material or seal degradation when cells were operated at 300 °C.

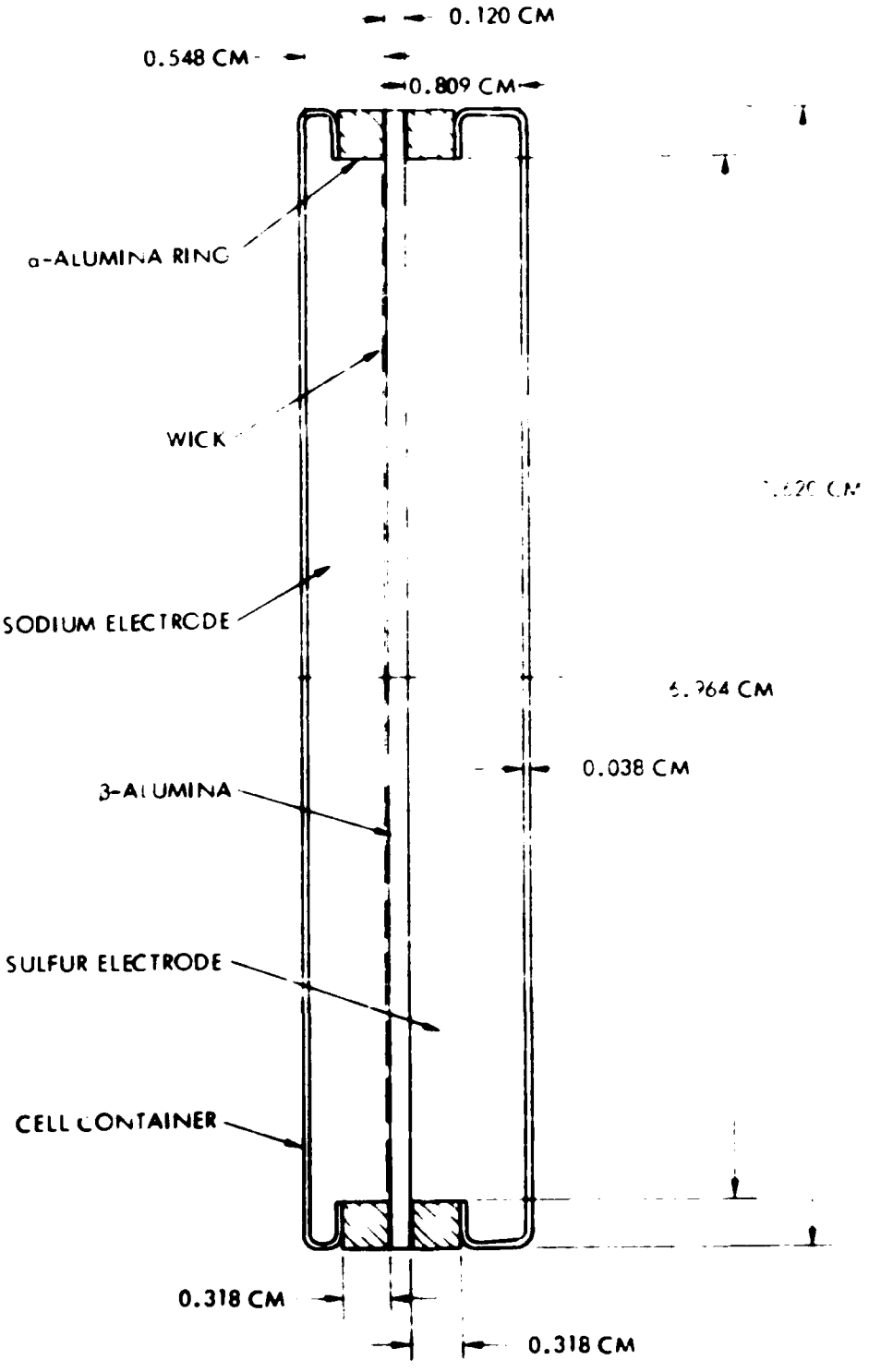

Figure 2-10. Schematic of 20-A hr Sodium-Sulfur Cell with Flat-Plate Electrolyte

- An electrolyte resistivity of 10 Ω cm at 300 °C was assumed based on improved solid electrolyte which has been fabricated at TRW.

- Internal resistance of the cell was presumed to be limited only by the ionic resistivity of the solid electrolyte.

- The electrolyte size (diameter and thickness) was selected to ensure mechanical integrity without any need for mechanical support.

- Electrolyte density of 3.24 g/cm^3 was selected as representative of solid electrolyte currently fabricated by a cold pressing and sintering process.

- The sulfur was impregnated into graphite felt (the graphite felt to sulfur ratio was 0.056 by weight), just as in the laboratory test cells, to provide electrical conduction within the cathode.

- The product of the net cell reaction was assumed to be sodium trisulfide, Na_2S_3.

- The cathode volume accretion was accounted for by assuming that the maximum cathode volume required is equal to the total weight of active materials (sodium and sulfur) divided by a conservative density of 1.86 g/cm^3.

- The stainless steel container material thickness was assumed to be 0.0381 cm (0.015 in.). This thickness of material can be formed readily into the required geometry with the required mechanical properties.

- Stainless steel screen was used in the anode compartment to provide wicking of molten sodium for maintaining sodium in contact with the electrolyte surface regardless of cell orientation and depth of discharge.

The projected performance for the flat-plate baseline cell design is given in Table 2-5. The specific energy requirement was easily satisfied and exceeded 100 W hr/kg. The main difficulty was to meet the required specific power. Specific power is the major performance characteristic affected by cell design. Specific power is written as

$$P_s = I(E - IR)/W_T$$

were I, E, R, and W_T represent delivered current (10 A), open-circuit cell voltage (2.08 V), internal cell resistance, and cell weight, respectively. The total cell weight, W_T, is a function of design capacity, electrolyte geometry, and cell configuration. The internal resistance of the cell, R, is a function of electrolyte resistivity and geometry, and of the operating temperature of the cell. For example, if the electrolyte thickness is

changed from 0.120 to 0.100 cm, the specific power increases from 112 to 118 W/kg for an electrolyte with a resistivity of 10 Ω cm at 300 °C. The effect of electrolyte resistivity on specific power for a single cathode cell is given in Figure 2-11. The specific power of a cell can be increased by:

- Reducing cell weight by changing the capacity, electrolyte geometry, or cell configuration
- Reducing electrolyte resistivity by changing the electrolyte fabrication process or formulation
- Reducing the resistance of the electrolyte by decreasing its thickness and increasing its area or by increasing the operating temperature of the cell.

The component weights for the baseline cell design, which are shown in Table 2-6 indicate that roughly one half of the total cell weight is in the container (can and α-alumina ring) and that the α-alumina rings account for 25% of the container weight. Therefore the elimination of the α-alumina rings will reduce the total container weight and increase the cell's specific power.

Table 2-5. Projected Characteristics and Performance Data for 20-A hr Sodium-Sulfur Baseline Cell

Total Cell Weight, g	158
Effective Area, cm^2	38.3
Internal Resistance, Ω	0.031
Capacity Density, A hr/cm^2	0.52
Maximum Current, A	33
Current Density, A/cm^2	0.86
Specific Power, W/kg	218
W/lb	99
Specific Energy, W hr/kg	263
W hr/lb	120
Performance at 10-A discharge (design point)	
Operation Voltage, V	1.77
Current Density, A/cm^2	0.26
Specific Power, W/kg	112
W/lb	51
Specific Energy, W hr/kg	224
W hr/lb	102
Cell Density, g/cm^3	2.2

Table 2-6. Weight Distribution for 20-A hr Baseline Cell Design

Component	Weight, g		Percent of Total	
Sodium	19.7		12.5	
Sulfur	41.2		26.1	
Electrolyte	17.7		11.2	
Felt	2.3		1.5	
Can - anode	28.2	76.7	17.9	48.7
- cathode	30.1		19.1	
Alumina Rings	18.4		11.7	
TOTAL	158		100	

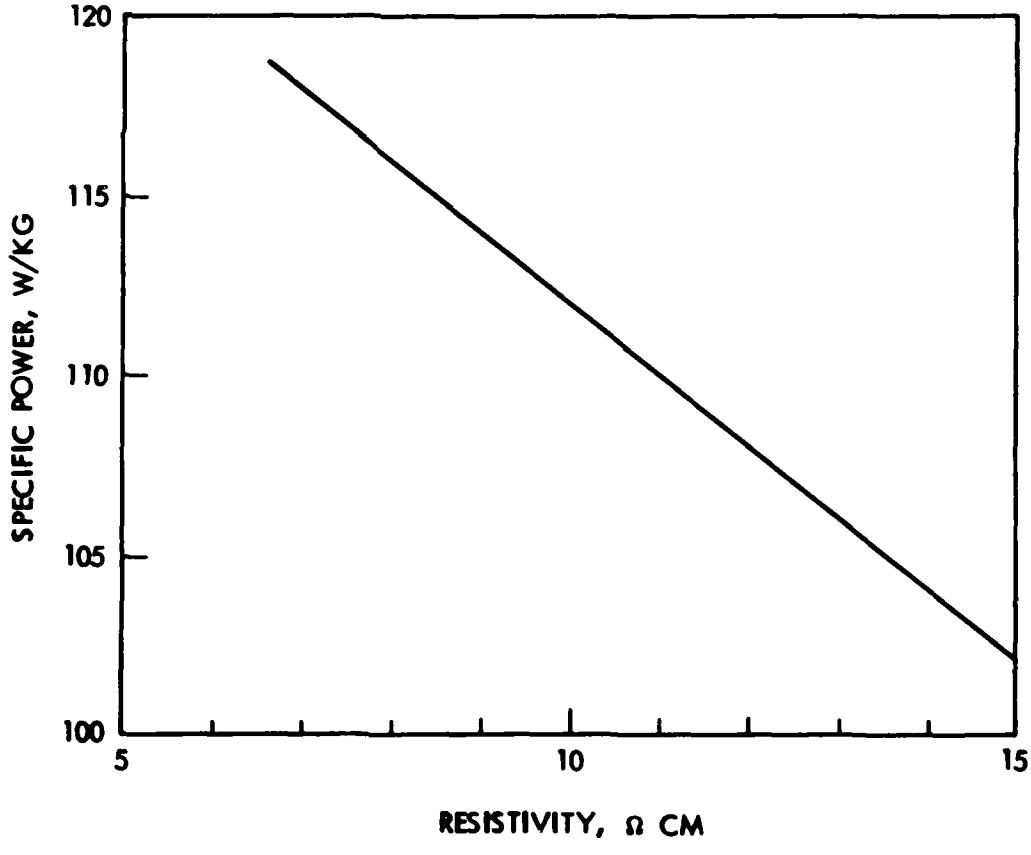

Figure 2-11. Effect of Resistivity on Specific Power of Baseline Cell at 10-A Discharge Design Point

2.6 Fabrication of Battery

2.6.1 Design Changes. The cell as shown in Figure 2-10 is a baseline design and was used to determine the engineering specifications and to project the cell performance. The cells that were actually fabricated, Figure 2-12, were based on these specifications and incorporate modifications in the baseline design to ensure safe, economical and timely construction. The expanded view in Figure 2-13 shows the various components of the cell.

The electrolyte was a 7.6-cm diameter magnesium oxide-enriched β-alumina disk fabricated by uniaxial precompaction followed by isostatic pressing and sintering. In order to minimize introduction of microcracks (from grinding) which can reduce mechanical strength, the electrolyte diameter was not ground to fit the α-alumina rings. The as-sintered electrolyte had a thickness of about 0.3 cm and was ground to a thickness of about 0.15 cm to remove possible sodium-depleted surface layers and surface irregularities and to provide flat surfaces for the α-alumina-to-β-alumina seals. The design thickness was 0.120 cm. The increase in electrolyte thickness resulted in a 25% increase in resistance, and the strength (maximum loading) of the electrolyte was doubled since the strength increases as the square of the electrolyte thickness.

The α-aluming rings were cut to 0.3-cm length from a tube which had a nominal 7.6-cm (3.0-in.) diameter and a 0.3-cm (0.125-in.) thick wall. All the rings were cut from the same tube and ground flat on both sealing surfaces. In order to minimize cost and time; no attempts were made to obtain the exact dimensions required from the design analysis or to grind the inner and outer diameters of the tube to remove noncircularity.

The cell container materials were 0.038-cm (0.015-in.) thick Kovar and Type 430 stainless steel. The Kovar which is part of the cell container was hermetically sealed to the α-alumina rings by seals of a conventional type used in high vacuum technology. The Kovar metal sleeve also provides a graded seal between α-alumina and the Type 430 stainless steel. Type 304 stainless steel could not be sealed to α-alumina directly by standard sealing techniques due to the large thermal expansion coefficient mismatch and therefore it was not used as a cell container material. Type 430 stainless steel was selected as an alternate to Type 304 stainless steel because of its low thermal expansion coefficient and good weldability even though it could not be directly sealed to the α-alumina.

The weld ring/cover plate configuration as shown in Figure 2-12 was used rather than a single piece container configuration as shown in the baseline design (Figure 2-10) in order to: 1) provide access to the cell interior during sealing, 2) provide maximum opportunity for inspection of the β-alumina and the seals, and 3) eliminate filling of the cell with both sodium and sulfur in the molten state. Filling only the anode (sodium) in the molten state eliminated the possibility of reaction between molten sodium and molten sulfur in the event of electrolyte failure. The sulfur cathode was prepared in pellet form and simply dropped into place after the anode had been filled with molten sodium and the cell had cooled to room temperature. The Type 430 stainless steel weld ring was laser welded

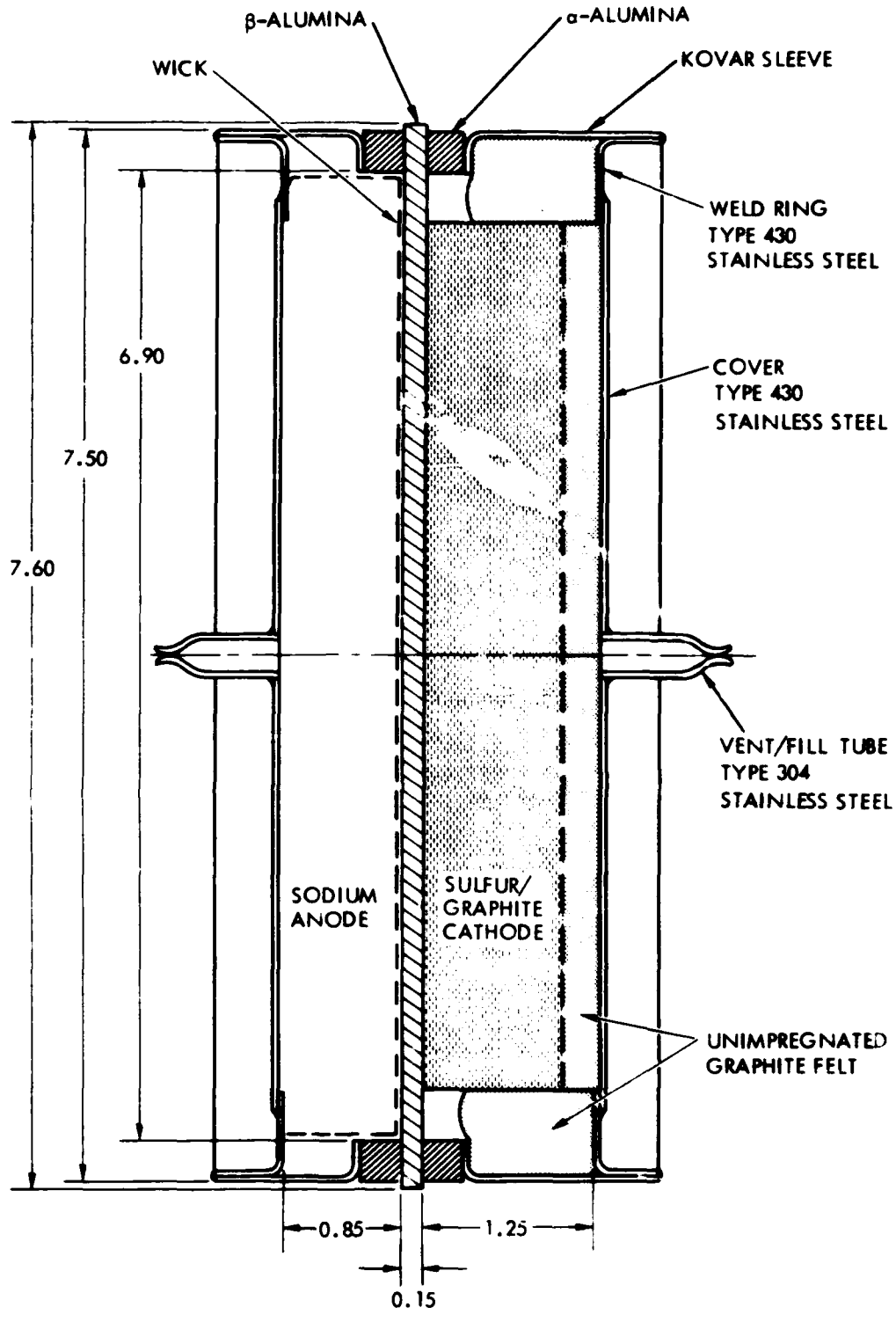

Figure 2-12. Schematic of Actual Cell.
Dimensions are in centimeters.

Figure 2-13. Expanded View of 20-A hr Hermetically Sealed Sodium-Sulfur Cell

to the Kovar metal sleeve in a butt configuration. This weld configuration allowed adjustment of the thicknesses of individual cell compartments in order to maintain the cell compartment volumes constant in spite of variations in fabricated and purchased parts, provided ease of welding without need for elaborate jigging and fixtures and closure tolerances, provided maximum distance between the metal-to-α-alumina seal and the weld (i.e., minimized heat transfer to the metal-to-ceramic seal), and allowed for thermal expansion differences between the Kovar sleeve and cell cover. The weld ring also allowed a continuous coating of protective chromium to be made over the Kovar surface and the exposed edges of the metal-to-ceramic seal.

Vent/fill tubes of nominal 0.32-cm (0.125-in.) o.d. Type 304 stainless steel were laser welded to the cell cover and were used for filling the anode side with molten sodium, for helium-leak checking the cell during fabrication, and for evacuating both sides of the cell before final closure. The cover plates were lap welded to the weld rings by means of a laser welding technique. The vent/fill tube closures were made by a technique in which the tubes were simultaneously pinched off and resistance welded.

Both compartments were identical in construction except for volume (i.e., thickness). The anode and cathode compartments were typically 0.85-cm and 1.25-cm thick, respectively. These thicknesses are greater than those of the baseline design of 0.55- and 0.81-cm for anode and cathode compartments, respectively. The anode compartment length was increased to allow ease in the application of the chromium plasma coating to the interior

walls and to provide some distance between the weld zone and the metal-to-ceramic seal. The cathode compartment length was increased for ease of application of the chromium coating, to provide adequate volume for a cathode pellet of simple goemetry, and to allow for a layer of unfilled felt required for compressing the pellet against the electrolyte surface to ensure good physical contact. The annular space between the metal-to-ceramic seal and weld ring was packed with unfilled graphite felt.

A sodium wick in the form of stainless steel mesh, Figure 2-14, was inserted in the anode compartment to provide maximum contact of sodium with the electrolyte surface at any cell orientation. The wick was made from 120-mesh Type 304 stainless steel screen. Several small stainless steel tabs, made from the same material, were spot welded to the screen to hold the wick flat against the electrolyte surface and to aid in the transfer of sodium to the wicks.

The internal surfaces of the Kovar sleeve, Type 430 stainless steel weld ring, and the metal-to-ceramic seal were plasma sprayed with chromium as a protection against corrosion due to sodium, sulfur and sodium polysulfides. Chromium was selected as the coating material rather than molybdenum, since recent compatibility studies by other investigators (S.A. Weiner, "An Overview of the Sodium-Sulfur Battery," SAE Automotive Engineering Congress and Exposition, 24-28 February 1975, Detroit, Paper 750149) have shown that under a static condition (no applied potential) Mo, Al, Zn, Ti, Ta and Cr are all compatible with sulfur and sodium polysulfide. At cell operating temperatures, with applied potentials, chromium is the only material that exhibits electrochemical behavior compatible with

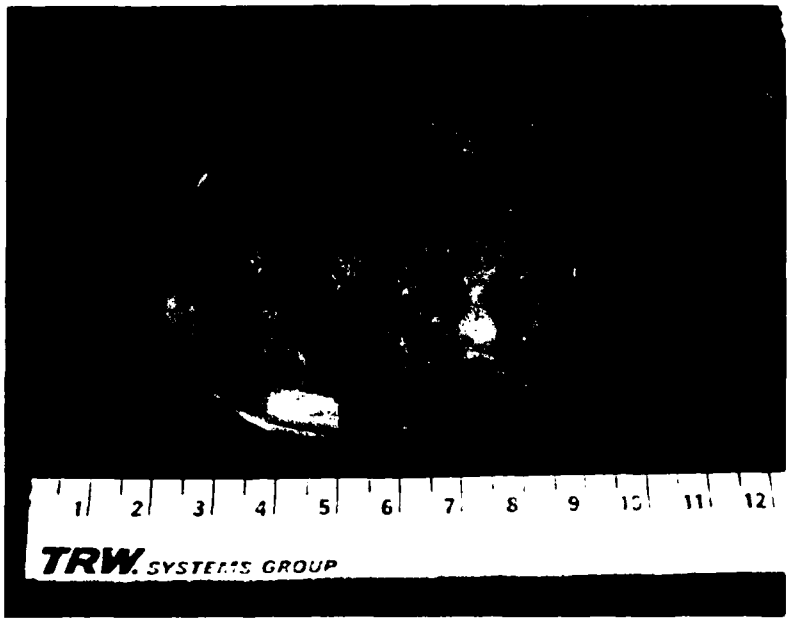

Figure 2-14. Sodium Wick

the polysulfide. In addition, the solubility of chromium sulfide has been shown to be low in melts of sodium polysulfide. The schematic in Figure 2-15 depicts the various seals and welds used in the actual cell.

2.6.2 Fabrication and Assembly Techniques. The basic steps involved in the fabrication of the 20-A hr cell were:

- o Fabrication of solid electrolyte
- o Fabrication of cell container components
- o Sealing of the solid electrolyte to the cell container
- o Final assembly, activation and hermetic closure of cell.

The detailed manufacturing flow diagram (Figure 2-16) indicates the steps involved in the fabrication process.

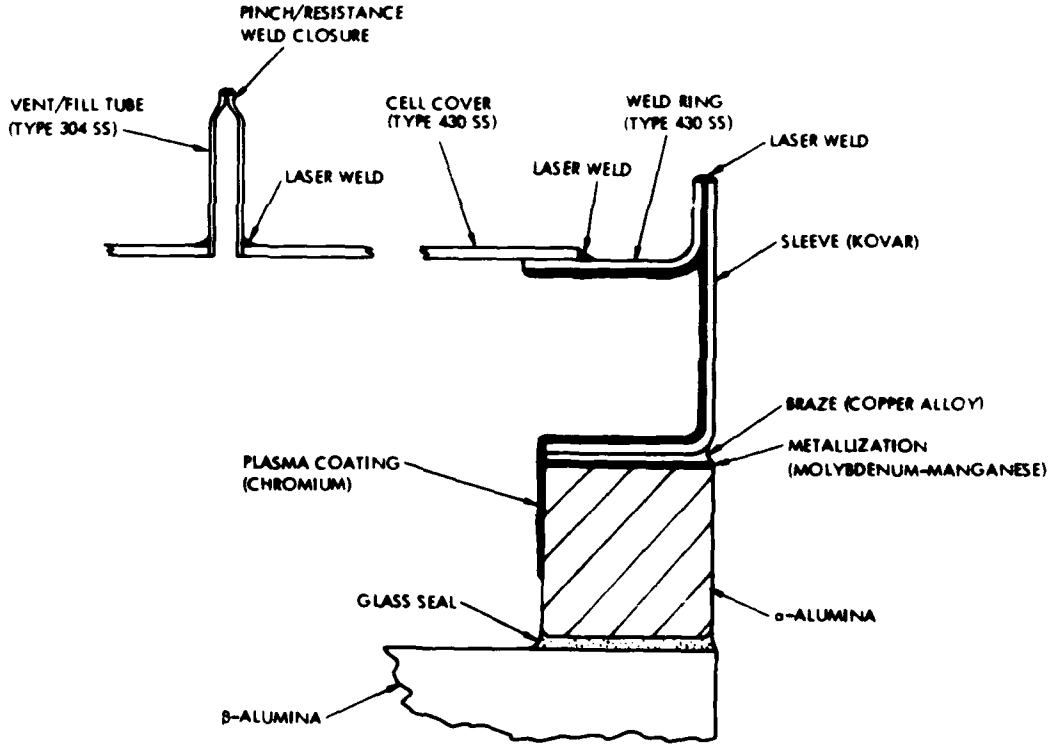

Figure 2-15. Schematic of Seals Used in Hermetically Sealed Cell

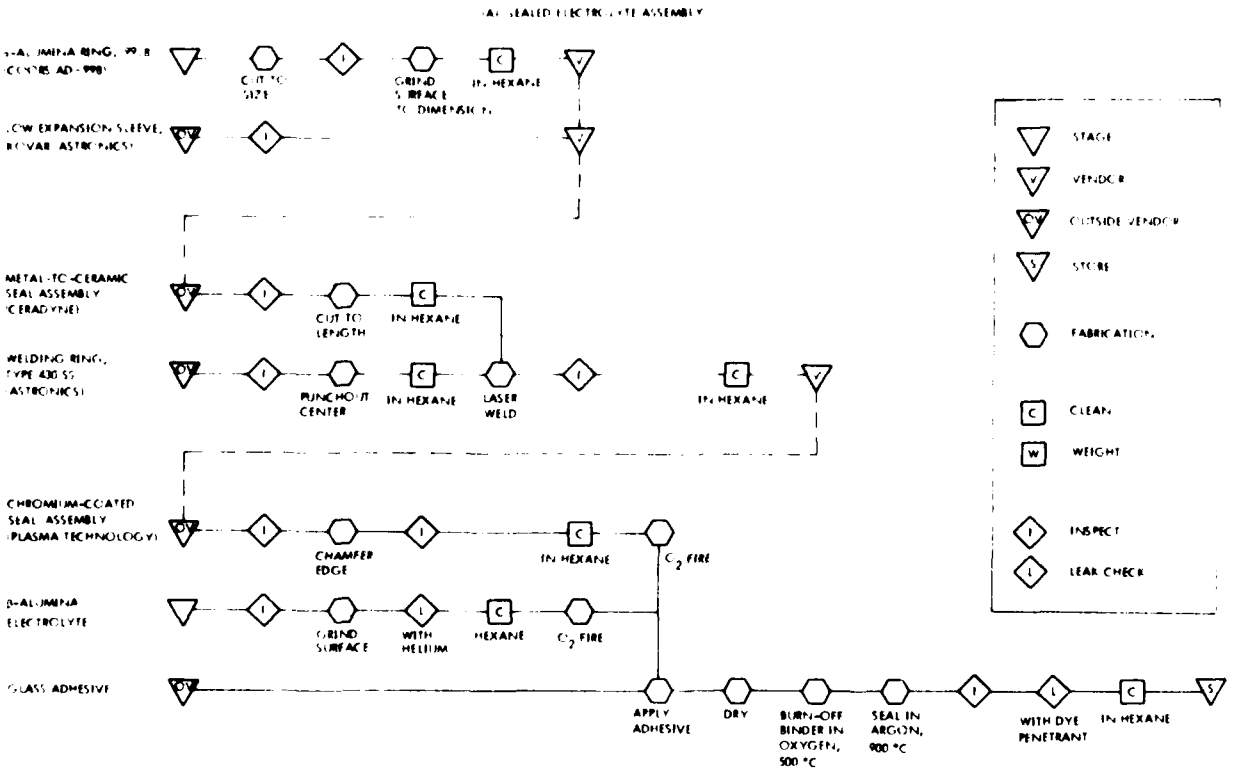

Figure 2-16. Manufacturing Flow Diagram

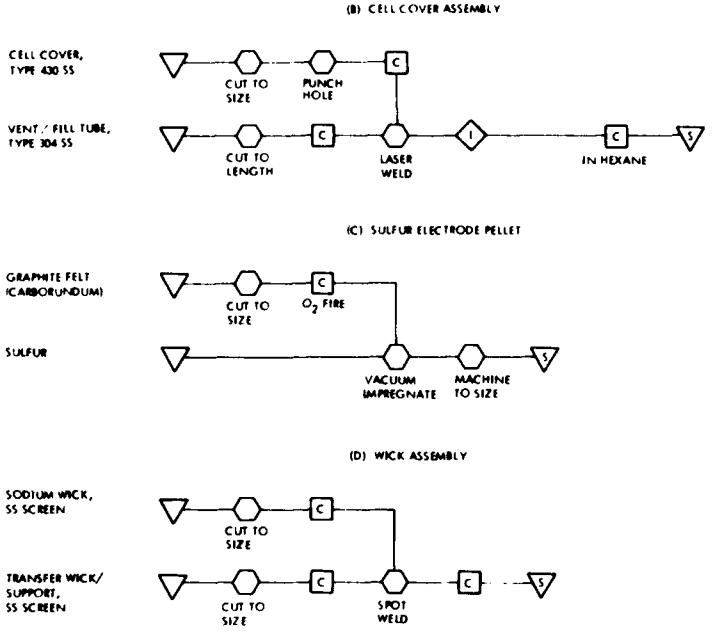

Figure 2-16. Manufacturing Flow Diagram (continued)

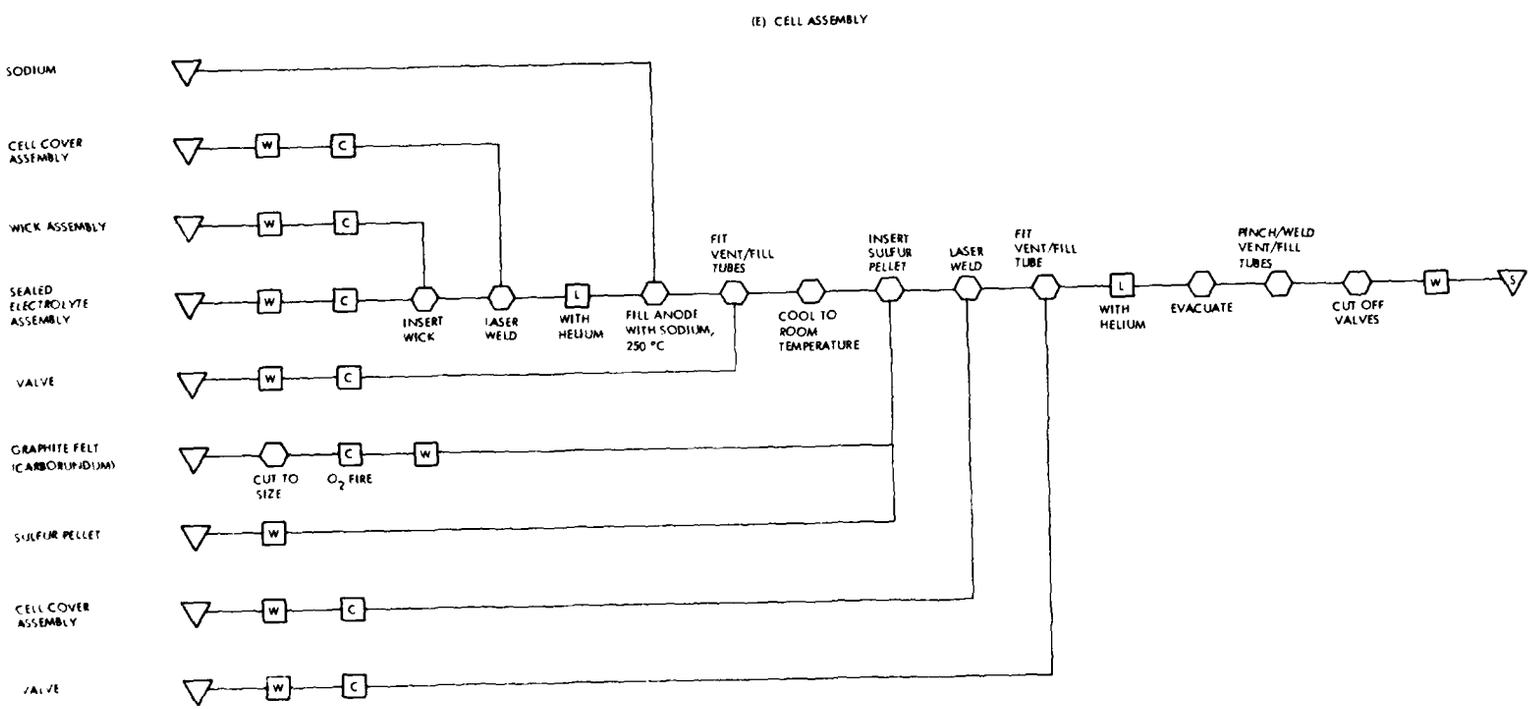

Figure 2-16. Manufacturing Flow Diagram (continued)

2.6.2.1 Solid Electrolyte. The magnesium oxide-enriched β-alumina electrolyte was fabricated by uniaxial precompaction and isostatic pressing followed by sintering. The as-sintered electrolytes typically had a 7.6-cm diameter, were 0.3-cm thick, and had a density of 3.24 g/cm^3. The electrolytes were visually inspected for cracks and flaws. A dye penetrant and strong transmitted light were used to facilitate detection of any irregularities in the electrolyte. The electrolytes were then surface ground to a final electrolyte thickness of 0.15 cm using a 70-μm diamond grit wheel with mineral spirits coolant. After the second visual inspection (with the aid of dye penetrant and transmitted light), the electrolytes were helium-leak checked, ultrasonically cleaned in hexane, and fired in oxygen at 950 °C for 4 hr to remove any residual organic contaminants.

2.6.2.2 Cell Container Components. The cell container components are the metal-to-ceramic seal, the weld ring, and the cell cover with vent/fill tube. The anode and cathode compartments are identical except for their thickness.

The metal-to-ceramic seals shown in Figure 2-17 were made by attaching a low thermal expansion Kovar sleeve to the end of the β-alumina ring in a butt configuration. The 0.4-cm long 99.8% β-alumina rings were cut from a nominal 7.6-cm diameter "off-the-shelf" tubing (Coors, AD-998) with 0.3-cm wall thickness. The rings were visually inspected for cracks and flaws before surface grinding to the final length of 0.3 cm. The low thermal expansion Kovar sleeve was fabricated by Astronic Co. (Pasadena, California) by spinning a 0.038-cm thick sheet stock into a short cylinder

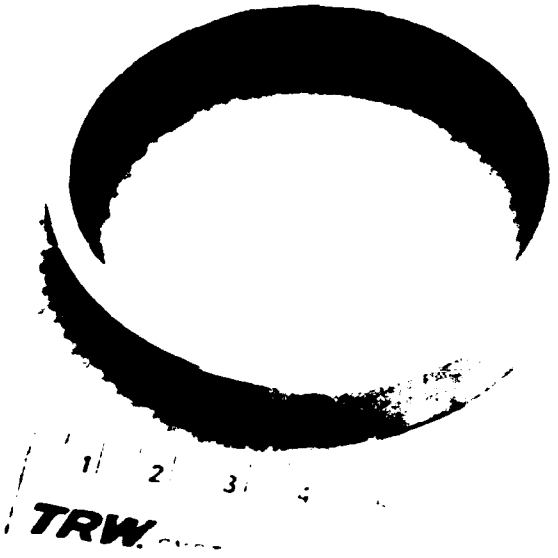

Figure 2-17. Metal-to-Ceramic Seal Assembly with Chromium Plasma Spray Coating

with a right angle flange facing inward on one end as shown in Figure 2-18. The sleeve was attached to a α-alumina ring at Ceradyne, Inc. (Santa Ana, California) by a standard molybdenum-manganese sealing technique used in high vacuum technology. This technique involves applying molybdenum-manganese metallization to one end of the α-alumina ring, electroplating and metallized surface with copper, and furnace brazing of the Kovar sleeve to the metallized surface with copper alloy braze.

The weld ring shown in Figure 2-18 was fabricated by punching out a disk from the bottom of a shallow cup spun at Astronic Co. from a 0.038-cm thick Type 430 stainless steel. The cups were spun to slip fit into the Kovar sleeve. Prior to butt welding the weld ring onto the Kovar sleeve by the laser welding technique, the sleeves were cut to the length required to provide the necessary volume for each of the cell compartments. The total inside lengths (including the α-alumina ring) for the anode and cathode compartments were 0.85 and 1.25 cm, respectively.

The metal-to-ceramic seal assembly shown in Figure 2-17 (α-alumina Kovar sleeve, and weld ring) was chromium coated by plasma spraying by Plasma Technology, Inc. (Torrance, California). The internal surface of the assembly except for one half the length of the α-alumina ring was grit blasted with alumina grit to remove surface contaminants and plasma coated to 0.013-cm thickness using -140- to +325-mesh 99.9% chromium (Metco)

The circular cell covers shown in Figure 2-19 were cut from 0.051-cm thick Type 430 stainless steel to such a diameter that a lap weld could be made to the weld ring. A 0.32-cm hole was punched in the center of the cover for attachment of the 0.32-cm (0.125-in.) diameter Type 304 stainless steel fill/vent tube by laser welding.

2.6.2.3 Sealed Electrolyte Assembly. The β-alumina electrolyte was sealed to the metal-to-ceramic seal assembly by means of a glass sealant. The sealant was applied to the α-alumina rings of the metal-to-ceramic assembly by means of a syringe. The assembly was positioned onto the electrolyte surface and allowed to dry in a forced convection oven at 110 °C for at least 4 hr. The second metal-to-ceramic assembly was then attached in an identical manner to the opposite side of the electrolyte. Any excess sealant was carefully removed from the electrolyte and the inside of the ring so that a small fillet remained. The electrolyte assembly was weighted down to provide a positive compressive force on the sealant and placed in furnace equipped with a retort. The sealing schedule involved heating at 25 °C/hr to 500 °C under flowing oxygen to provide an oxidizing environment for organic solvent burnout, continued heating at 25 °C/hr in a flowing inert (argon) atmosphere to the sealing temperature of 950 °C, maintaining a static inert atmosphere at 950 °C for 3.5 hr, and cooling at 25 °C/hr in a static inert atmosphere to room temperature. Total furnace time was 72 hr. The sealed electrolyte assemblies were checked visually with aid of a dye penetrant for leaks and cracks.

2.6.2.4 Final Assembly, Activation and Closure. The fabrication of the anode compartment was completed by insertion of the stainless steel

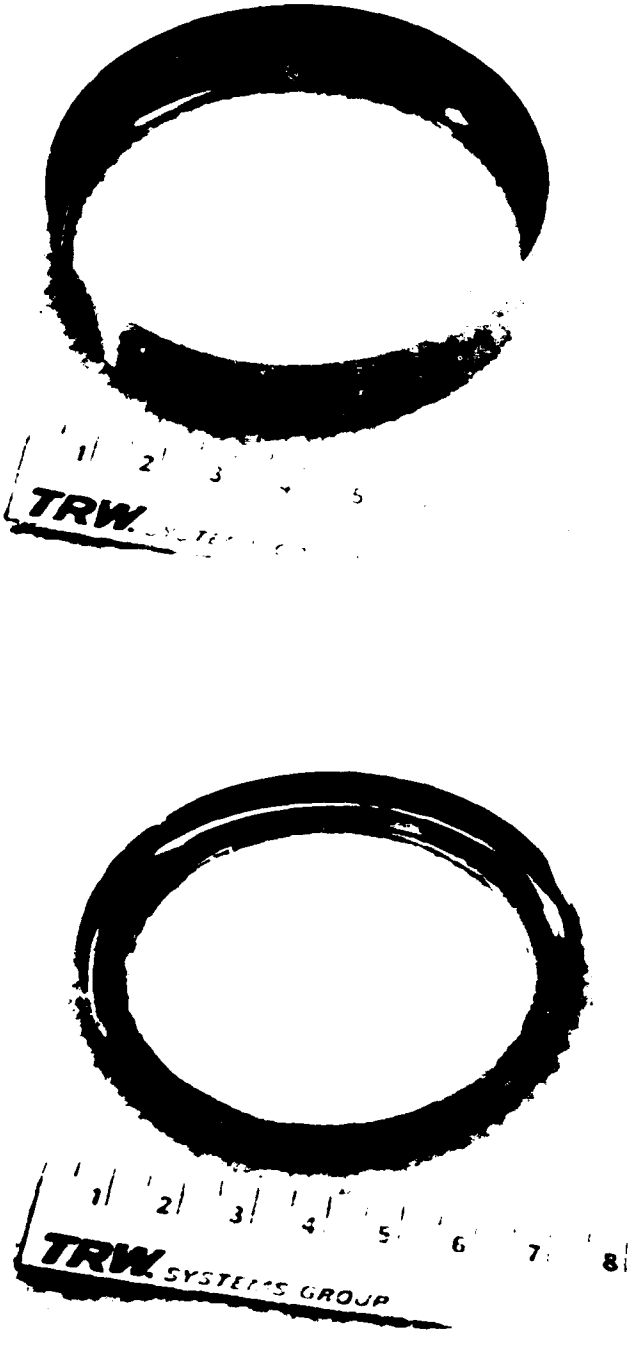

Figure 2-18. Cell Container Components. Top, Kovar sleeve; bottom, Type 430 stainless steel weld ring.

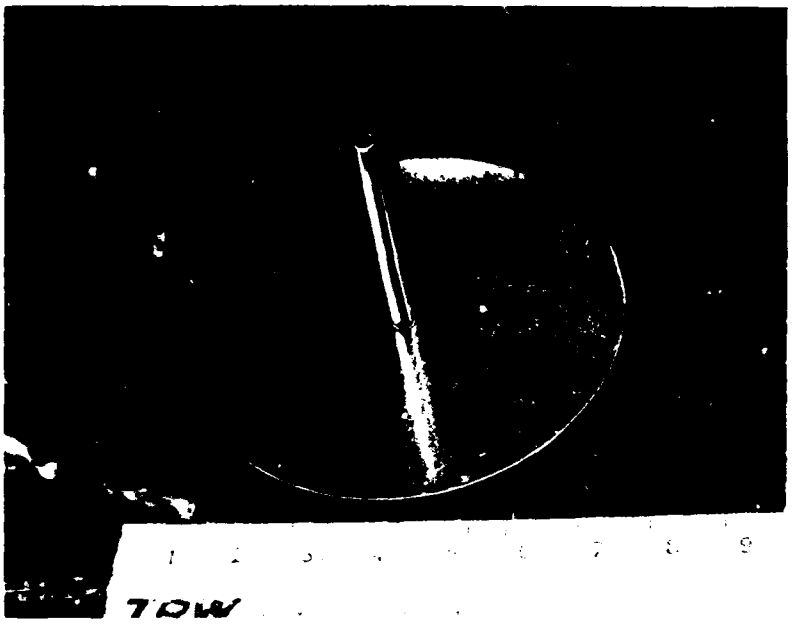

Figure 2-19. Cell Cover-Vent/Fill Tube Assembly

sodium wick and laser welding the cover plate to the anode assembly weld ring. All of the seals in the anode compartment were then helium-leak checked. The partially completed cell shown in Figure 2-20 was placed in a special heating fixture inside the inert atmosphere chamber and heated at about 30 °C/hr to 250 °C. The sodium reservoir was also heated to 250 °C and the anode compartment was filled by gravity flow through the vent/fill tube. The vent/fill tube was closed with a valve after cooling the cell (30 °C/hr) to ambient temperature. The amount of sodium in the cell was determined by weight difference.

The final assembly and activation of the cell were carried out under ambient conditions. As annular shaped piece of unfilled graphite felt was placed between the α-alumina ring and the weld ring of the cathode compartment. The cathode sulfur pellet, fabricated by vacuum impregnation of graphite felt with molten sulfur, was positioned in the cathode compartment backed up by a layer of unfilled graphite felt to provide a slight compression on the pellet. A cover plate was laser welded to the weld ring and the vent/fill tube was closed with a valve. All the seals in the cathode compartment were then helium-leak checked.

A hermetic closure of the cell was made after evacuation of both anode and cathode compartments by simultaneously crimping and resistance welding to provide increased reliability in the hermetic closure. A photograph of the completed cell is shown in Figure 2-21.

Figure 2-20. Partially Completed Cell. Anode compartment ready for sodium filling.

2.6.3 Fabricated Cells. Six (6) hermetically sealed cells were fabricated out of fifteen cells attempted. Eight cells were not completed due to failures attributable to the seal between the α-alumina ring and the β-alumina disk and the electrolyte of one cell cracked while the anode assembly was being filled with sodium. Four cells have been delivered untested to USAECOM, Fort Monmouth, New Jersey. One of the remaining two cells has undergone thermal and electrical cycling in accordance to the Technical Guidelines and its test results are discussed in the Section 2.7 Figures 2-21 and 2-22 show a photograph and X-ray views, respecitvely, of the four deliverable cells (Cells No. 4, 5, 9, and 10).

The weight distribution of the cells, Table 2-7, shows that even though the percentage weight distribution of components is essentially the same as the baseline design, Table 2-6, the actual weight of the components has increased. These increases are attributable in general to the modifications made to allow timely and economical fabrication of the deliverable cells.

The cell capacity was determined by the amount of sodium present in the anode compartment which depended on the conditions during the gravity-fed filling step (surface tension of sodium, wettability of cell components, temperature, and the sodium reservoir head pressure). No attempts were made to reproduce the filling conditions for each cell. The amount of sodium dispensed at 250 °C is shown in Table 2-7. The total anode volume for the cells based on actual dimensions is 45.3 cm^3 corresponding to a

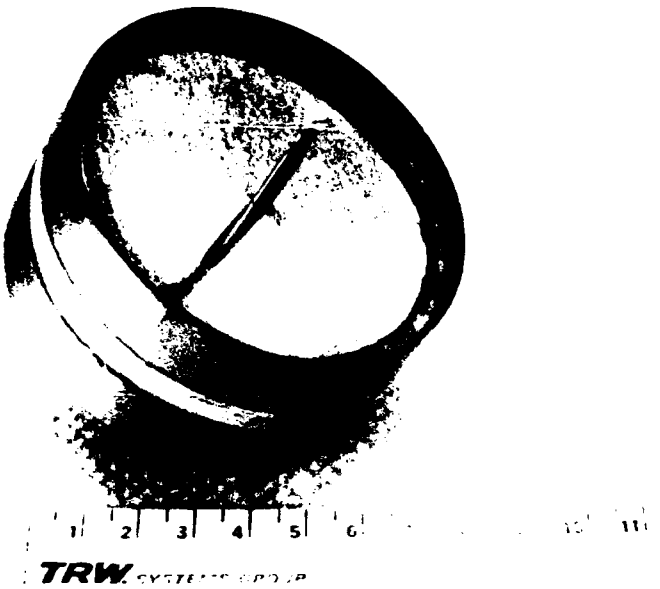

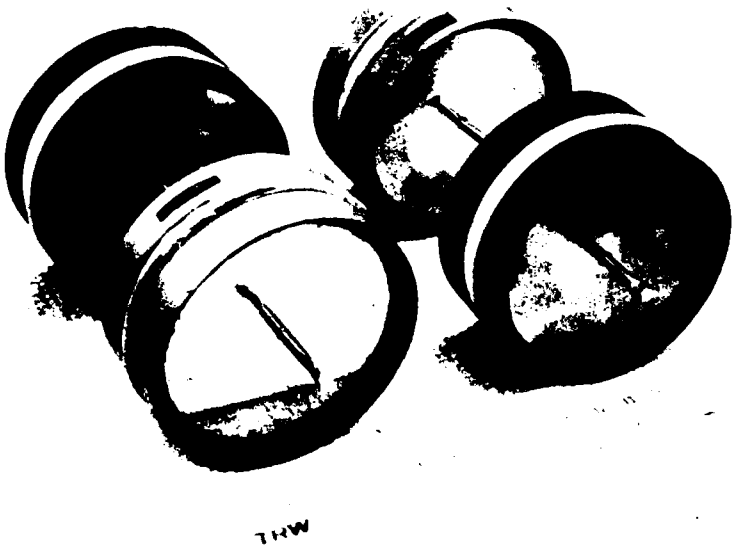

Figure 2-21. Photographs of Hermetically Sealed 20-A hr Sodium-Sulfur Cells. Top, single cell; bottom, four deliverable cells.

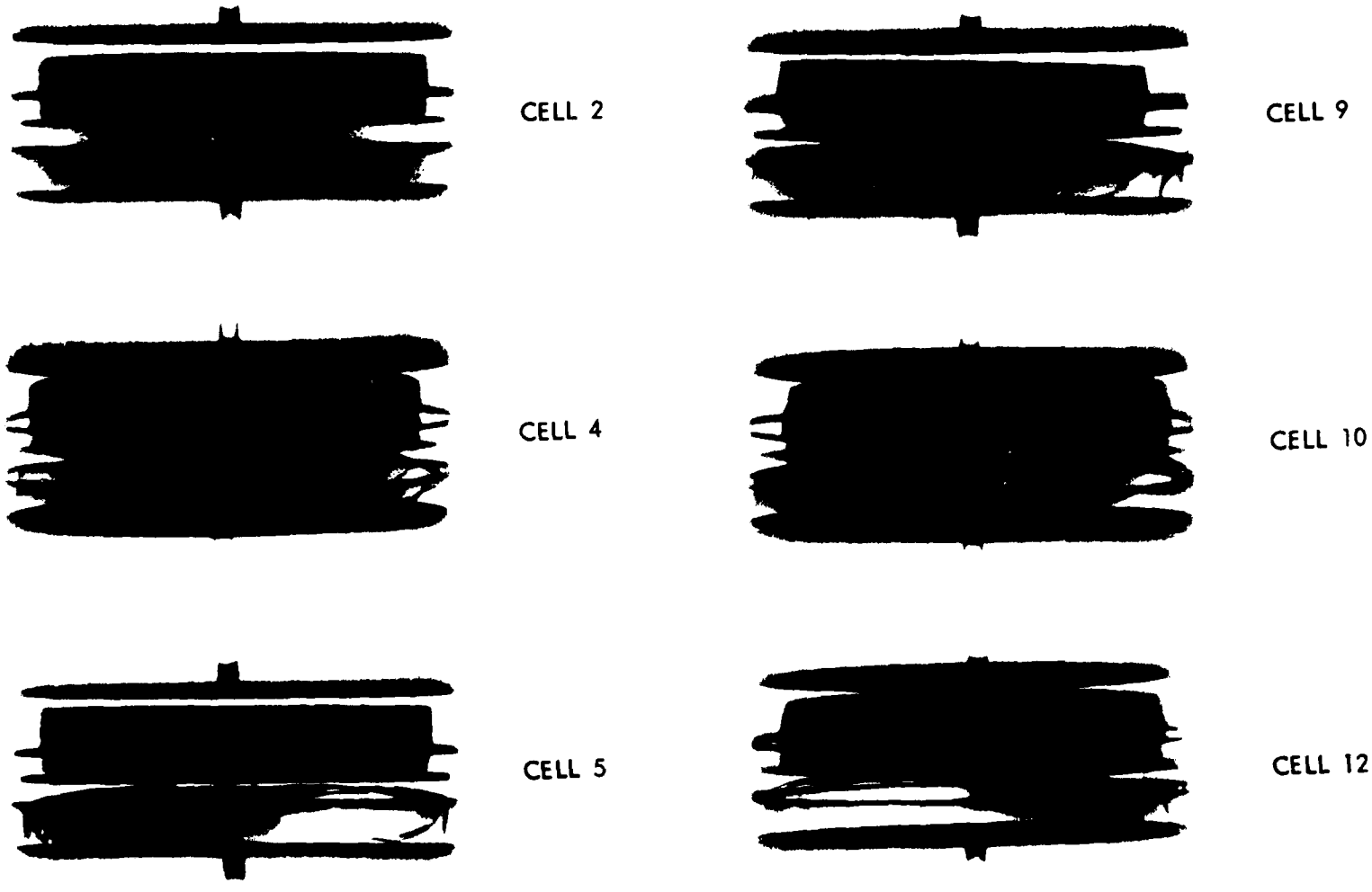

Figure 2-22. X-Ray Photograph of the Completed Cells

Table 2-7. Weight Distribution of Hermetically Sealed Cell Components (in grams)

	Cell Number					
	2	4	5	9	10	12
Sodium	33	21	21.3	24.3	23.8	22.6
Sulfur	50	51.4	49.7	47.8	49.4	50.1
Electrolyte	17.2	21.5	21.7	22.1	22.1	22.3
Felt	3.6	3.5	3.6	3.8	3.9	3.9
Wick	--	2.2	2.2	2.2	2.2	2.2
Container	86	84.4	79.5	91	89	79
Complete cell	190	184	178	191	190	180
Excess Weight	32	26	20	33	32	22

capacity of 47 A hr. This volume is not completely filled with sodium because of nonwetting of cell components at 250 °C and entrapped gases as evident from the X-ray photographs shown in Figure 2-22.

If the cell capacity were based on the actual dimensions of the cell as shown in Figure 2-12, it would be limited by the sulfur electrode. That is, capacities based on the dimensions of anode and cathode compartments are 47 and 44 A hr, respectively. The capacity of the sulfur electrode actually used in the cells, Table 2-7, is about 28 A hr. Therefore, the amount of sulfur present is more than adequate to satisfy the 20-A hr cell requirements. The void volume in the cathode resulted from the need to insert the cathode electrode into the cathode compartment in a preformed pellet. This meant that the sulfur electrode pellet had to be of simple right cylindrical geometry with a diameter less than the inside diameter of the weld ring. The void volume of the unfilled graphite felt used to provide slight compressive force against the sulfur pellet and that placed in the annular space between the weld ring and α-alumina ring is more than sufficient to allow for volume increase of the cathode due to discharge.

2.7 Evaluation of Battery. The evaluation of the battery consisted of testing cells or cell components against the performance characteristics specified in Paragraph 2 of the Technical Guidelines for the Investigation of High Temperature Battery Systems and was carried out in two parts. In the first part a boiler-plate cell was used to evaluate full-size components of the cell, such as the 7.6-cm diameter β-alumina electrolyte, wick, and α-alumina-to-β-alumina seal. A hermetically sealed cell representative of those fabricated for delivery to USAECOM was used in the second part of

the evaluation to test the validity of the design with respect to the performance goals.

2.7.1 Boiler-Plate Cell. A boiler-plate cell was constructed to evaluate full scale components of the hermetically sealed cell under actual cell operating conditions. Specifically, the components evaluated were: α-alumina-to-β-alumina seal, stainless steel screen for sodium wick, 7.6-cm diameter β-alumina electrolyte, and sulfur cathode (sulfur-impregnated graphite felt). In addition, evaluations were made on the double ring-disk seal configuration, and the effect of orientation on cell operation.

2.7.1.1 Cell Assembly. The double ring-disk assembly was made with a uniaxially pressed and sintered magnesium oxide-enriched β-alumina electrolyte sealed to 7.6-cm o.d. α-alumina rings (Coors, AD-998) which had a 0.635-cm square cross section. The glass seal has made by heating in air at 850 °C for 4 hr. The electrolyte and the double ring-disk assembly were leak tight to helium.

The sodium wick was made from a 120-mesh Type 304 stainless steel screen. Three small pieces of the screen rolled into cylinders (0.8-cm o.d. by 1.2-cm long) were spotwelded equally spaced onto the wick to act as springs for maintaining positive contact between the wick and the electrolyte surface.

The cathode sulfur pellet was made by vacuum impregnation of sulfur (Mallinckrodt) into graphite felt (Carborundum). The felt was cleaned by firing at 500 °C for 1 hr in vacuo prior to sulfur impregnation. After sulfur impregnation, the pellet was machined to final size.

All parts of the boiler-plate cell except for the cathode sulfur pellet and sodium wick were degreased in hexane. The sodium wick was cleaned using Freon followed by acetone and hexane. One side of the preheated double ring-disk assembly was filled with sodium by placing a small amount of molten sodium on the electrolyte surface, putting the wick in place and filling above the wick with additional sodium. The assembly was kept at 350 °C to allow sodium wetting of the electrolyte and wick. After cooling the assembly, sodium chips were added to complete the filling.

Assembly of the boiler-plate cell was completed by placing the sulfur pellet backed by an unfilled layer of felt in the cathode side of the double ring-disk assembly, gasketing each side with Grafoil (Union Carbide) gaskets and bolting the boiler plates together with insulated bolts. The bolts were torqued to 8.5 in. lb. Both sides of the assembly were then evacuated. The cell was heated at a rate of 15-20 °C/hr by means of circular heater plates taped to the boiler plates. The cell was maintained at an operating temperature of 345 °C. Cell heat-up was carried out with the electrolyte in the horizontal position and the sodium side up. Figures 2-23 and 2-24 are a schematic showing the expanded view of the cell and a photograph of a fully assembled boiler-plate cell, respectively.

2.7.1.2 Cell Testing and Results.

(a) Stainless Steel Wick. - The effectiveness of a stainless

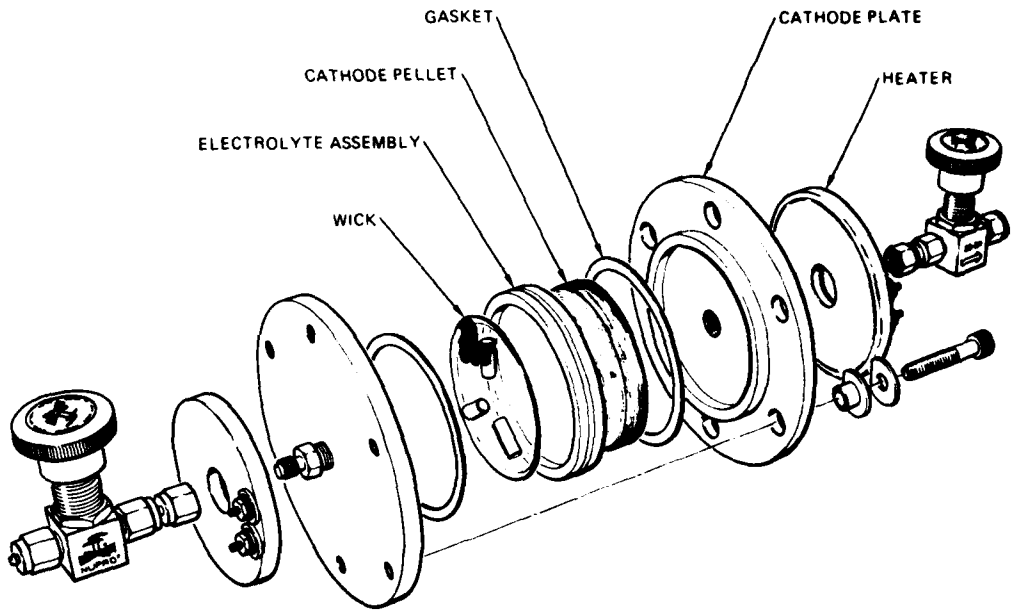

Figure 2-23. Expanded View of Boiler-Plate Test Cell

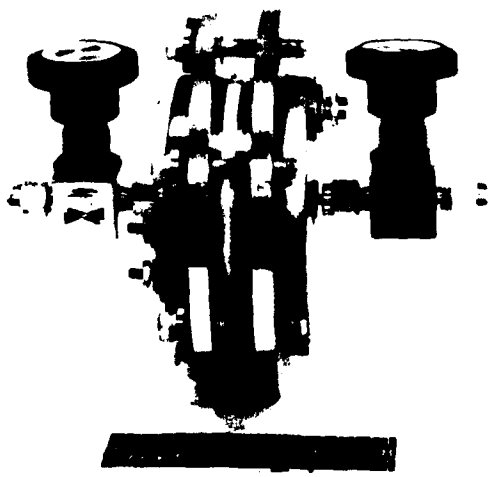

Figure 2-24. Fully Assembled Boiler-Plate Cell

steel screen for sodium wicking was checked by noting the internal resistance of the cell in various cell orientations. Initially the cell was maintained at open circuit with the sodium side up for 72 hr at 345 °C to allow adequate time for sodium wetting of the electrolyte and screen. Resistance measurements were made with the cell in this position, and then with 1) the sulfur side on top, 2) the electrolyte positioned vertically, and 3) the cell finally returned to its initial sodium-side up position. Each position was held for approximately 0.5 hr. No change in cell resistance was observed as a function of cell orientation which indicated that the stainless steel screen maintained a constant area of contact between sodium and the electrolyte. Post-test examination of the wick revealed fair wetting of the stainless steel. The appearance of the screen was in general clean except for areas containing dark deposits, Figure 2-25.

(b) Orientation Effect on Performance. The effect of cell orientation on performance related to mass transfer and/or density gradients in the sulfur cathode was investigated. The cell was positioned with the sodium anode on top and allowed to equilibrate at open circuit. It was then discharged at 2 A for a total of 4 A hr

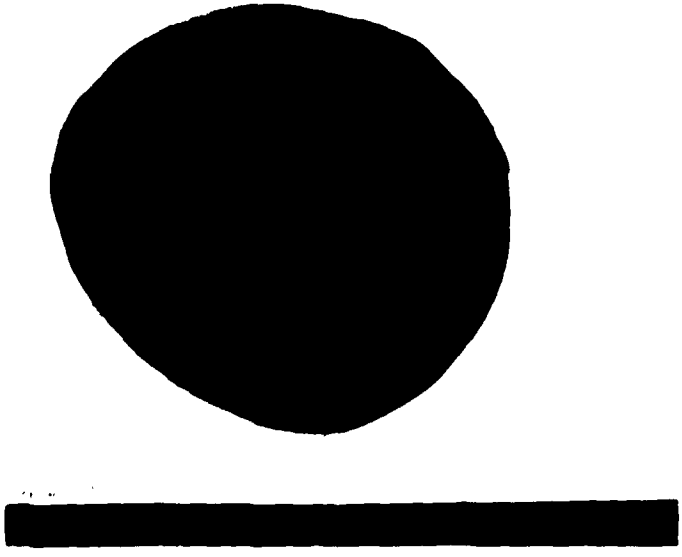

Figure 2-25. Post-Test Photograph of Sodium Wick

which represented approximately 50% depth of discharge. After leaving the cell at open circuit for 15 hr, it was charged at 2 A for a total of 2 A hr before voltage limiting. The cell was then inverted so that the sulfur cathode was on top and allowed to equilibrate at open circuit. Further charging of the cell at 2 A was unsuccessful with only 0.2 A hr being passed before reaching the voltage-limited condition. Subsequent discharging and charging at 2 A was at 100% coulombic efficiency with a passage of 2 A hr in each direction. The results of this test were inconclusive in determining the effect of cell orientation on its performance.

(c) Electrical Performance. In order to determine its electrical performance, the cell was cycled several times at a constant current of 2 A followed by discharging and charging at various constant currents. The results are summarized in Table 2-8. The cell was discharged at a constant current of 2 A in Cycle No. 7, until the cell voltage decreased rapidly with time indicating utilization of all available sodium. Discharge of the cell after the twelfth cycle resulted in the cell voltage immediately dropping to less than 0.5 V indicating possible loss of cell capacity due to an external short. The cell was charged at a constant current of 2 A for 5 hr before voltage limiting. Cycle No. 13 verified recharging of the cell. After Cycle No. 14, a sudden decrease in open-circuit cell voltage to less than 0.3 V was observed and cell testing was terminated. The total charge passed in each direction was 50 A hr with an overall coulombic efficiency of 100%. If the cell capacity (as determined by Cycle No. 7) is taken as about 6 A hr, the cell underwent total of 8 turnovers based on sodium. The total test time was 480 hr at 345 °C.

The polarization behavior of the cell is shown in Figure 2-26. The initial resistance determined from polarization data was 0.34 Ω compared to 0.48 Ω measured by an AC milliohmmeter. A polarization curve measured after Cycle No. 13 indicated a cell resistance of about 0.12-0.16 Ω which agreed with the value determined by the AC milliohmmeter. Linearity in the polarization curves indicates resistive behavior of the cell even at 10-A discharge (300 mA/cm^2).

During disassembly of the cell, a possible external short caused by leakage of sulfur from the Grafoil gasket was observed. Bridging of the sulfur/polysulfide to the sodium anode boiler plate can lead to a small electrical short which in turn would explain

Table 2-8. Summary of Electrical Performance Testing of Boiler-Plate Cell

	Discharge Period		Charge Period		
Cycle	Current, A	Charge, A hr	Current, A	Charge, A hr	Coulombic Efficiency, %
1	2	4	2	1.9*	52
			2	0.2	
2	2	2	2	2	100
3	2	4	2	3.5	88
4	2	4	2	3.8	95
5	2	4	2	4	100
6	2	4	2	4	100
7	2	5.8	2	5.4	93
8	4	4	4	3.6	90
9	6	4	6	4	100
10	8	4	8	4	100
11	10	4	4	4	100
12	2	4	2	6.4	160
13	2	0.06	2	0.06	100
					90
14	2	1.3	2	3.9	300
Total		49.1		49.7	

*Sodium anode up

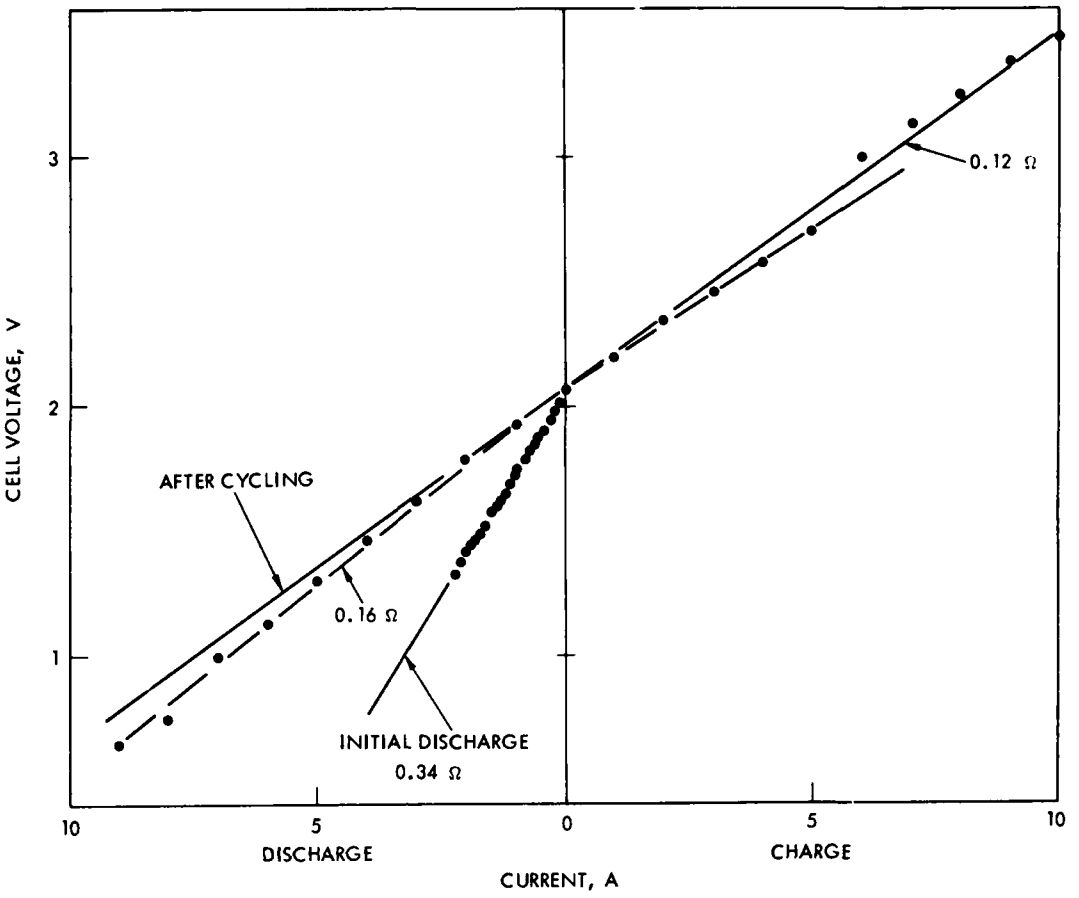

Figure 2-26. Polarization Curves for Boiler-Plate Test Cell

the inability of the cell to retain its charge. The sudden decrease in open-circuit voltage probably was caused by a small pinhole through the electrolyte. Post-test examination of the electrolyte revealed holes through the electrolyte due to delamination as shown in Figure 2-27.

(d) Double Ring-Disk Seal. Post-test examination of the α-alumina ring-to-β-alumina disk seal indicated no degradation or leakage of the seal after 480 hr of operation at 345 °C. The seal material as well as the double ring-disk configuration appeared to be good. Results from other tests carried out for the Electric Power Research Institute revealed that the double ring-disk assembly can be subjected to thermal cycling without seal failure.

Figure 2-27. Post-Test Photograph of Electrolyte Assembly Showing Sulfur Electrode Side

2.7.2 Test Plan. The performance goals for the hermetically sealed cells are 50 W/lb and 50 W hr/lb for specific power and specific energy, respectively, with a capacity of 20 A hr when discharged at the 2-hr rate to a cut-off voltage of 1.0 V with a coulombic efficiency of no less than 90% through 100 charge-discharge cycles.

A test plan was developed based on the Technical Guidelines. It incorporated five (5) thermal cycles and 100 electrical cycles. The thermal cycles involved cooling from an operating temperature of about 310 to 25 °C in 30 hr (∿10 °C/hr), followed by reheating to operating temperature in 10 hr (∿30 °C/hr), maintaining at operating temperature for 24 hr and discharging at the 2-hr rate. The electrical cycles included a 10-A discharge for 2 hr to a cut-off voltage of 1.0 V followed by a 4-hr charge at 5 A with a 2.5-V cut-off. Total test time (including thermal cycles) was estimated to be 1000 hr.

The performance testing was carried out using a cell test station which was identical to those used in our previous effort except that the bell jar was evacuated rather than filled with argon. In this way, the bell jar not only provided a protective barrier in the event of catastrophic cell failure, but also allowed visual observation of the cell since no thermal insulation was necessary to prevent heat loss (i.e., the vacuum acted as a thermal insulator).

2.7.3 Hermetically Sealed Cell.

2.7.3.1 Cell Assembly. A hermetically sealed cell of the design shown in Figure 2-12 was tested to evaluate its performance characteristics. The cell contained 33 g of sodium and 50 g of sulfur. Therefore, the cell capacity was limited by the sulfur electrode to 32 A hr. The total cell weight was 190 g (exclusive of the heaters). The anode compartment did not contain any wick and a small pinhole in the α-alumina-to-β-alumina seal on the cathode side was patched with a high temperature ceramic adhesive. The cell was helium-leak checked prior to final closure and found to be leak tight. The completed cell is shown in Figure 2-28.

2.7.3.2 Cell Testing and Results. The cell was placed on the test stand with the electrolyte in a horizontal position as shown in Figure 2-29. Since the cell did not contain any wick, the sodium side was on top during the first 10 cycles to ensure wetting of the entire electrolyte surface. Plate heaters were held in place on each end of the cell with a U-shaped clamp and bolt arrangement. A thick disk of insulative ceramic was used between the heaters and the cell to provide electrical insulation while maintaining a good thermal path. A heat-up rate of about 15 °C/hr was used to heat the cell from room temperature to the operating temperature of 310 °C. The internal resistance of the cell was monitored with an AC (1 kHz) milliohmmeter. The electrical cycle testing was done with a TRW-designed cell tester similar to those used in the previous effort.

2.7.3.3 Internal Resistance. The initial open-circuit cell voltage was 2.09 V at operating temperature. With the sodium side up the cell resistance as measured with the AC milliohmmeter was 8.3 Ω. The DC resistance value measured from slope of the polarization curve shown in Figure 2-30 was measured by constant current and revealed a linear relationship between current and voltage which indicated the voltage drop to be purely resistive in nature.

Even though its high internal resistance prevented the cell from being discharged at high rates, while maintaining the voltage above 1.0 V, the cell was cycled by discharging at 0.5 A for 1 hr and charging for 3 hr (constant current of 0.16 A until voltage limit of 3.5 V followed by constant voltage charging). Since the internal resistance of the cell had not decreased appreciably after cycling (2.5 Ω after cycling), the cell was cooled to room temperature and inverted to bring the sulfur side on top. A polarization curve, Figure 2-29, with the sulfur side up revealed a linear relationship between current and voltage with two distinct slopes. The slopes were 0.48 and 0.29 Ω for low currents (less than 1.0 A) and high currents, respectively. In this position, the cell could be discharged at currents up to 3.0 A while maintaining the voltage above 1.0 V.

The resistance value required to maintain a cell voltage above the cut-off voltage of 1.0 V at a discharge rate of 10 A is 0.10 Ω or less. The calculated cell resistance based only on electrolyte resistance is 0.03 Ω. The source of the large cell resistance is not known at this time. However, it can be speculated to be due to poor electrical contact between current collector(s) and electrode(s), poor or inadequate sodium wetting, and blockage of the current collector surface by corrosion products or impurities.

Figure 2-28. View of Hermetically Sealed Cell No. 2. Top, before and, bottom, after performance testing.

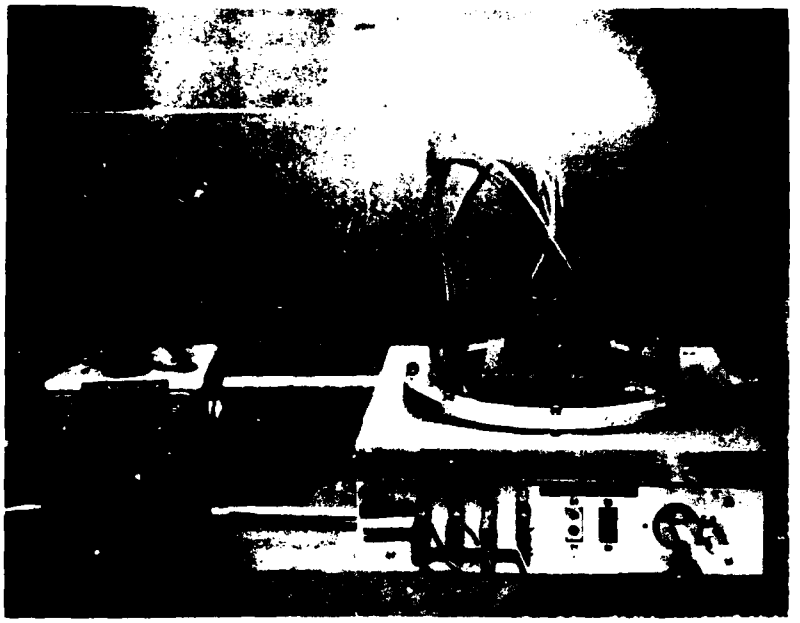

Figure 2-29. Hermetically Sealed Cell Undergoing Performance Testing

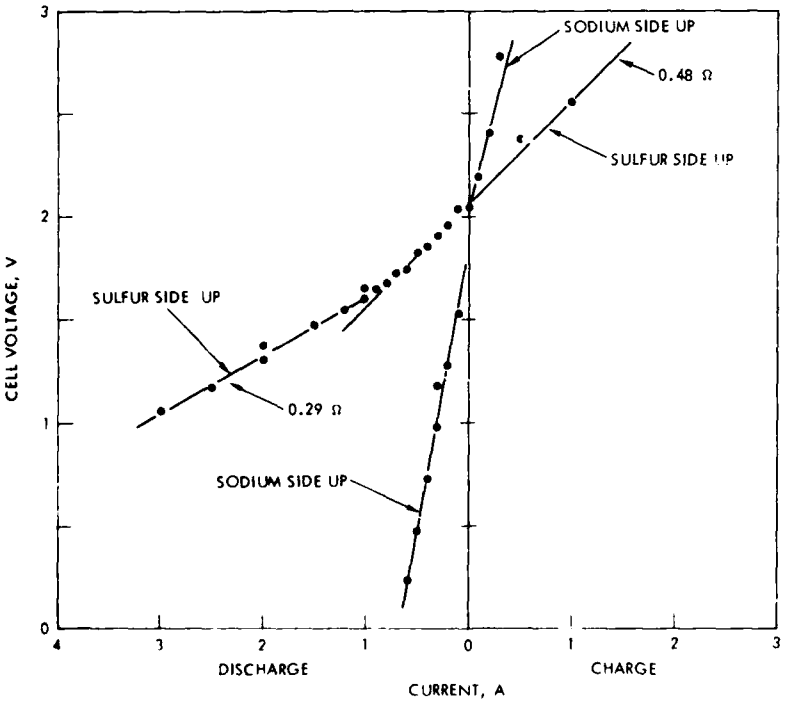

Figure 2-30. Polarization Curve for Cell No. 2

2.7.3.4 Electrical Cycling. The test plan called for electrical cycling by discharging at 10 A for 2 hr followed by charging at 5 A. Due to its large internal resistance, the cell could not be cycled at the required rate. However, limited cycling was carried out using charge and discharge rates up to 5 A. A coulombic efficiency of well over 90% was observed for 57 cycles performed over ∿800 hr. The electrical cycling is summarized in Table 2-9.

The maximum power point, from the polarization data with the sulfur side up, occurs at a current of 3 A. The corresponding specific power is 16 W/kg. The maximum specific energy for this cell is 310 W hr/kg. The specific energy increase is attributed to an increase in active material used in this cell (Cell No. 2). The decrease in maximum specific power is related to the increase in total cell weight due to increased active materials and to the increase in cell resistance.

2.7.3.5 Thermal Cycling. The large cell resistance prevented electrical cycling at the required 10-A rate. However, the cell was thermally cycled at a rate higher than that required by the Technical Guidelines. The cell was thermally cycled by cooling from the operating temperature of 310 °C to room temperature at a rate of 30 °C/hr followed by heating at the same rate to the operating temperature of 310 °C. The cell was held at open-circuit conditions for at least 12 hr before electrically cycling. Thermal cycling was conducted after electrical Cycle No. 10, 45, 48, 51 and 57. As can be seen from Table 2-9 the cell did not exhibit any degradation in performance after the thermal cycles. The appearance of the cell after testing is shown in Figure 2-28 and did not reveal any gross leakage.

Table 2-9. Summary of Results for Hermetically Sealed Cell (Cell No. 2)

	Discharge Period		Charge Period	
Cycle	Current, A	Charge, A hr	Current, A	Charge, A hr[a]
1-10[b,c]	0.5	5.5	0.16	2.8
11-12[d]	1.0	0.3	1.0	0.6
13	5.0	10.0	5.0	2.8
14-35	1.0	37.0	1.0	44.9
36-41	2.0	12.0	2.0	12.4
42-43	4.0	2.0	2.0	1.7
44-45	4.0	2.0	4.0	2.4
46-48	4.0	5.7	4.0	3.8
49	1.0	0.5	1.0	0.5
50-51	4.0	2.0	4.0	1.6
52	0.1	0.1	1.0	0.2
53-56	5.0	4.0	3.0	2.8
57	5.0	2.0	5.0	1.5
Total		84.1		78.0

Capacity: 32 A hr (sulfur limited)

Total Weight: 190 g

Operating Temperature: 310 °C

---

[a] Includes charge passed during constant-voltage charging.

[b] Sodium electrode up. All other cycles with sulfur electrode up.

[c] Thermal cycling after Cycle No. 10, 45, 48, 51 and 57.

[d] Cycle No. 46-57, charge passed during constant-current charge only.

3. CONCLUSIONS AND RECOMMENDATIONS

Hermetically sealed sodium-sulfur cells were designed to meet or exceed the performance characteristics specified in Paragraph 2 of the Technical Guidelines for the Investigation of High Temperature Battery Systems. The cells utilized a disk-shaped magnesium oxide-enriched β-alumina electrolyte with a resistivity of 10 Ω cm at 300 °C and an effective surface area of 39 cm^2. Six such cells were fabricated and the feasibility of the design has been demonstrated.

The projected performance of the cell at a 10-A discharge rate is 112 W/kg and 224 W hr/kg for specific power and specific energy, respectively. However, due to high internal resistance, the cell could not be discharged at currents greater than 3 A while maintaining the operating voltage above 1.0 V. The cell has been electrically cycled for 57 cycles (over 800 hr) with a coulombic efficiency greater than 90% without any sign of performance degradation. In addition the cell has undergone five thermal cycles from operating temperature to room temperature and back to operating temperature without exhibiting any loss of performance. The maximum specific energy was 310 W hr/kg and the specific power at maximum power (3-A current) was 16 W/kg.

Cells built and tested to date have exhibited high internal resistance leading to failure of the cell to reach high discharge currents. The source of the large cell resistance is not known at this time. Post-test analysis is being carried out and additional cells are being tested in an attempt to learn the source of this high resistance. It appears that additional knowledge of the manufacturing processes as well as effects of impurities on cell performance is necessary for an understanding of the high resistance.

The design modifications and fabrication steps used in this program were necessary for timely and economical construction of the cells. The seal between the β-alumina electrolyte and cell container was based on state-of-the-art technology and no seal failures have been observed at operating temperatures. However, in order to lower cost and to eliminate the use of chemically incompatible materials such as Kovar and copper braze, further work in the seal area is suggested. Seal improvements can result from eliminating or decreasing the size of the α-alumina rings (which account for 12% of total cell weight), using an active metal braze, and directly sealing the metallic cell container to the β-alumina electrolyte.

The metallic container materials used in the present program were selected primarily for ease in making the α-alumina-to-metal seal and secondarily for chemical compatibility with the active materials. In the limited testing of a hermetically sealed cell, no cell failure due to the materials of construction has been observed. Nevertheless, for construction of long-life cells further work is necessary in development of cell container materials. Furthermore, effort should be expended to further characterize all materials of construction of the cell.

Finally, additional work is necessary to improve reliability and reproducibility of various manufacturing steps. Needed improvements include:

improvement of the reproducibility of filling the anode with sodium, increasing the yield in the fabrication of β-alumina-to-α-alumina seal, minimizing void volume in the cathode compartment, and reduction of the amount of laser welding.

DISTRIBUTION LIST

101 Defense Documentation Center
ATTN: DDC-TCA
Cameron Station (Bldg 5)
012 Alexandria, VA 22314

206 Commander
Naval Research Laboratory
ATTN: Library
001 San Diego, CA 92152

207 Commander
US Naval Ordnance Laboratory
ATTN: Technical Library
001 White Oak, Silver Sprg, MD 20910

210 Commandant, Marine Corps
HQ, US Marine Corps
ATTN: Code LMC
001 Washington, DC 20380

301 Rome Air Development Center
ATTN: Documents Library (TILD)
001 Griffiss AFB, NY 13441

307 HQ ESD (XRRI)
L.G. Hanscom Field
001 Bedford, MA 01730

408 HQDA(DARD-ARS-P/Dr. R.B. Watson)
001 Washington, DC 20310

442 Commander
Harry Diamond Laboratories
ATTN: Library
2800 Powder Mill Road
001 Adelphi, MD 20783

483 Commander
US Army Research Office
ATTN: AMXRO-IP
PO Box 1221
001 Research Triangle Park, NC 27709

486 Commander
US Army Mobility Eqpt R&D Ctr
ATTN: SMEFB-R
001 Fort Belvoir, VA 22060

488 US Army Security Agency
ATTN: IARD
Arlington Hall Station
001 Arlington, VA 22212

680 Commander
US Army Electronics Command
Fort Monmouth, NJ 07703

1 AMSEL-TL-DT
1 AMSEL-TL-P (Ofc of Record)
2 AMSEL-MS-TI
1 AMSEL-GG-TD
1 USMC-LNO
32 AMSEL-GG-AR

703 NASA Scientific & Tech Infor Facility
ATTN: Acquisitions Branch (S-AK/DL)
PO Box 33
002 College Park, MD 20740

HQDA (DAMA-CSC Major R.C. Baugh)
001 Washington, DC 20310

Mr. Don Mortel
Director, Aerospace Power Div.
ATTN: AFAPL/PO
001 Wright-Patterson AFB, Ohio 45433

Mr. E. Cohn
NASA Headquarters
Code RPP
001 Washington, DC 20546

Institute for Defense Analyses
ATTN: Mr. Robert Hamilton
PO Box 55
001 Libertytown, MD 21762

Commander
US Army Materiel Command
ATTN: AMCRD-FP
5001 Eisenhower Avenue
001 Alexandria, VA 22333

Commander
US Army Materiel Command
ATTN: AMCRD-TC
5001 Eisenhower Avenue
001 Alexandria, VA 22333

Commander
US Army Mobility Equipment R&D Center
ATTN: SMEFB-EE
001 Fort Belvoir, Virginia 22060

Commander
Harry Diamond Laboratories
ATTN: AMXDO-RDD (Mr. A. Benderly)
2800 Powder Mill Road
001 Adelphi, MD 20783

HQDA (DARD-DDC-C)
001 Washington, DC 20310

Commander
Picatinny Arsenal
ATTN: SMUPA-FR-SP (Mr. M. Merriman)
001 Dover, New Jersey 07801

Power Information Center
University City Science Institute
3401 Market Street, Room 2210
001 Philadelphia, Pennsylvania 19104

Office of Assistant Director
(Engineering Technology), ODDR&E
Rm 3D-1089 ATTN: Mr. R.W. Ziem
Pentagon
001 Washington, DC 20301

Mr. Richard E. Oderwals
Department of the Navy
Hqs., US Marine Corps
Code LMC 4
001 Washington, DC 20380

UNCLASSIFIED
SECURITY CLASSIFICATION OF THIS PAGE (When Data Entered)

REPORT DOCUMENTATION PAGE	READ INSTRUCTIONS BEFORE COMPLETING FORM
1. REPORT NUMBER: ECOM-74-0587-F	2. GOVT ACCESSION NO.	3. RECIPIENT'S CATALOG NUMBER: -26619-6013-RU-00
4. TITLE (and Subtitle): Investigation of High Temperature Battery Systems.	5. TYPE OF REPORT & PERIOD COVERED: Final Report 1 July 74 - 31 Aug 75
	6. PERFORMING ORG. REPORT NUMBER
7. AUTHOR(s): R.R. Sayano, M.L. McClanahan, J.A. Male, and N. Fried	8. CONTRACT OR GRANT NUMBER(s): DAAB07-74-C-0587
9. PERFORMING ORGANIZATION NAME AND ADDRESS: TRW Systems Group, TRW Inc. One Space Park Redondo Beach, California 90278	10. PROGRAM ELEMENT, PROJECT, TASK AREA & WORK UNIT NUMBERS: IS7 62705 A H94 P2-083
11. CONTROLLING OFFICE NAME AND ADDRESS: US Army Electronics Command AMSEL-TL-PG Fort Monmouth, New Jersey 07703	12. REPORT DATE: Dec 75
	13. NUMBER OF PAGES: 56 + vi
14. MONITORING AGENCY NAME & ADDRESS(if different from Controlling Office)	15. SECURITY CLASS (of this report): Unclassified
	15a. DECLASSIFICATION DOWNGRADING SCHEDULE

16. DISTRIBUTION STATEMENT (of this Report)

Approved for public release, Distribution Unlimited

17. DISTRIBUTION STATEMENT (of the abstract entered in Block 20, if different from Report)

18. SUPPLEMENTARY NOTES

19. KEY WORDS (Continue on reverse side if necessary and identify by block number)

High Temperature Battery
Sodium
Sulfur
Solid Electrolyte
Beta-Alumina
Hermetically Sealed Cell
Sodium-Sulfur Battery

20. ABSTRACT (Continue on reverse side if necessary and identify by block number)

Hermetically sealed sodium-sulfur cells intended to operate at 300 °C in atmospheric environment and to deliver 10 A for 2 hr above 1.0 V for 100 cycles with a specific power and specific energy of 110 W/kg and 110 W hr/kg, respectively, were designed and fabricated. The cells were to withstand five thermal cycles from operating temperature to room temperature without loss of electrical performance. These cells utilized a disk shaped magnesium oxide-enriched β-alumina electrolyte with low cost materials for cell containers.

DD FORM 1 JAN 73 1473 EDITION OF 1 NOV 65 IS OBSOLETE

UNCLASSIFIED
SECURITY CLASSIFICATION OF THIS PAGE (When Data Entered)

The seals used in the cell were all based on state-of-the-art technology and comprised a glass sealant between the β-alumina electrolyte and the α-alumina rings, copper braze between the α-alumina rings and the Kovar cell containers, and laser welds between the Kovar cell containers and the stainless steel cell cover. Chromium plasma coating was used to protect the copper braze and Kovar against corrosion by sulfur and/or sodium polysulfide. No catastrophic cell failure due to cell design or materials of construction has been observed during testing of a cell for over 800 hr.

A cell has been electrically cycled for 57 cycles (over 800 hr) with a coulombic efficiency greater than 90% without any sign of performance degradation. In addition the cell has undergone five thermal cycles from operating temperature to room temperature and back to operating temperature without exhibiting any loss of performance. The projected performance of the cell at the 10-A discharge rate is 112 W/kg and 224 W hr/kg for specific power and specific energy, respectively. However, due to high internal resistance, the cell could not be discharged at currents greater than 3 A while maintaining the operating voltage above 1.0 V. The maximum specific energy was 310 W hr/kg and the specific power at maximum power (3-A current) was 16 W/kg.